

Figure 5.3. Electric field distribution plots due to 0.04 Hz MMT plane wave source for the background and 1-D reservoir models.

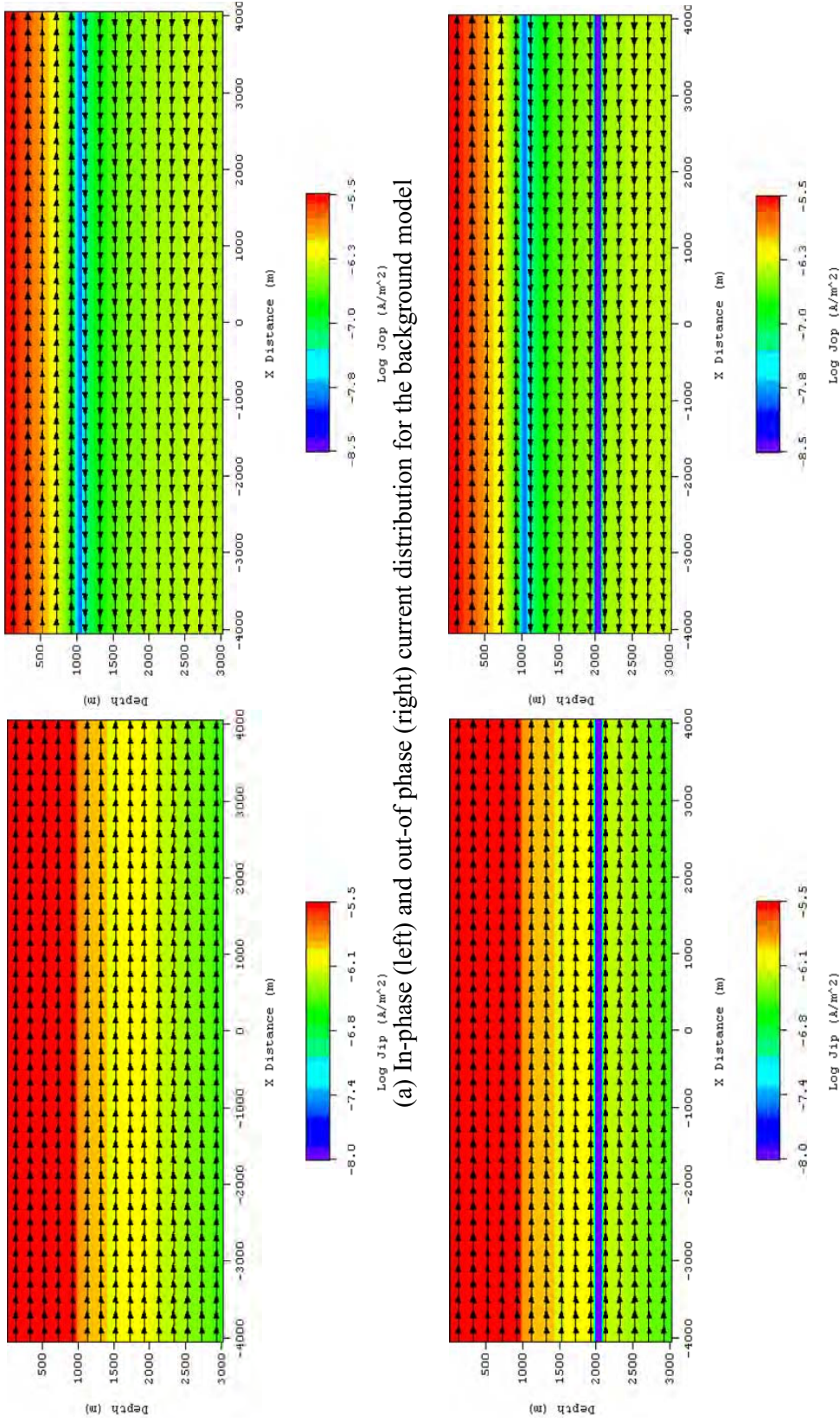
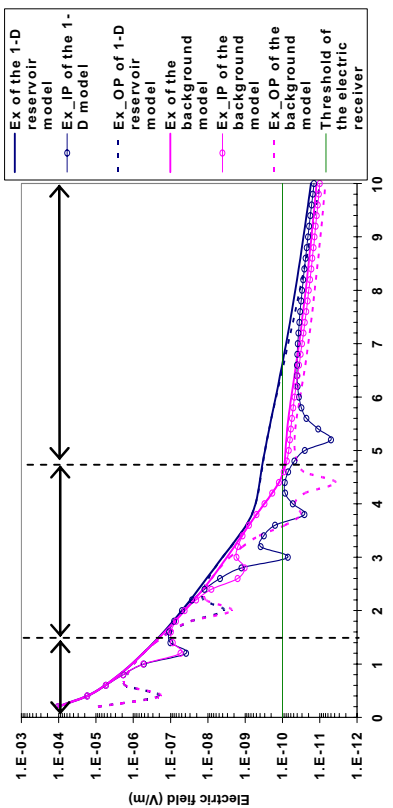
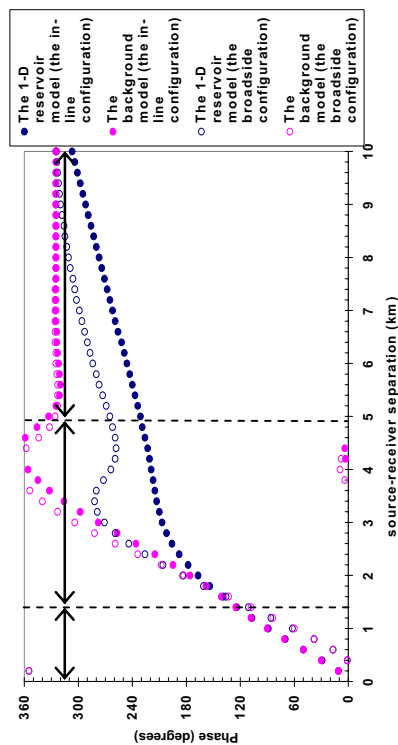


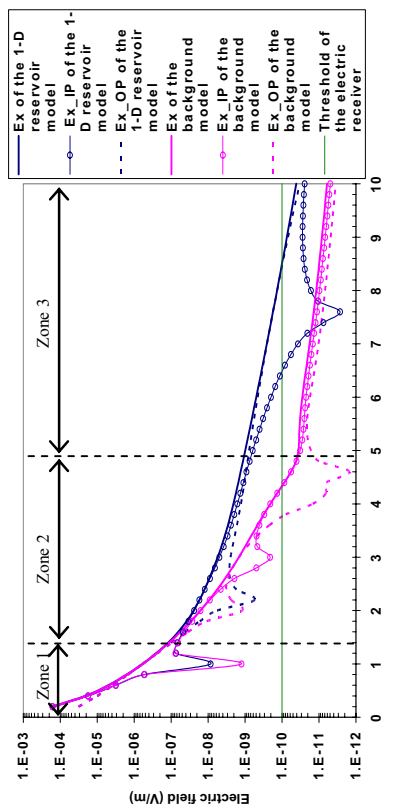
Figure 5.4. Current distribution plots due to 0.04 Hz MMT plane wave source for the background and 1-D reservoir models.



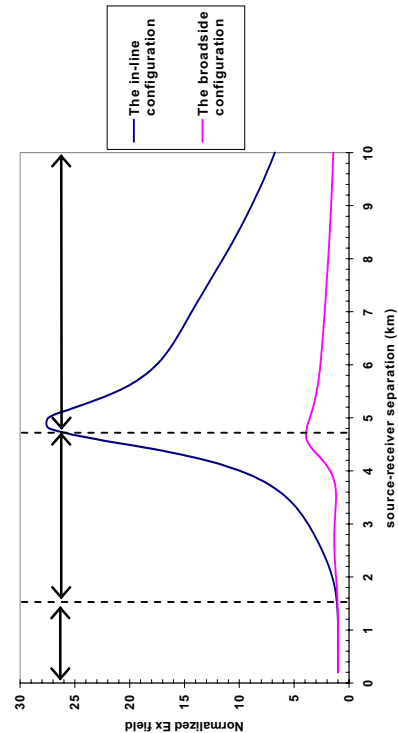
(a) The in-line Ex responses



(c) The phases of the Ex components



(b) The broadside Ex responses



(d) The normalized Ex responses

Figure 5.5. Ex responses at 0.63 Hz for the background and 1-D reservoir models. The partition of the left plots is based on the in-line responses and that of the right the broadside responses.

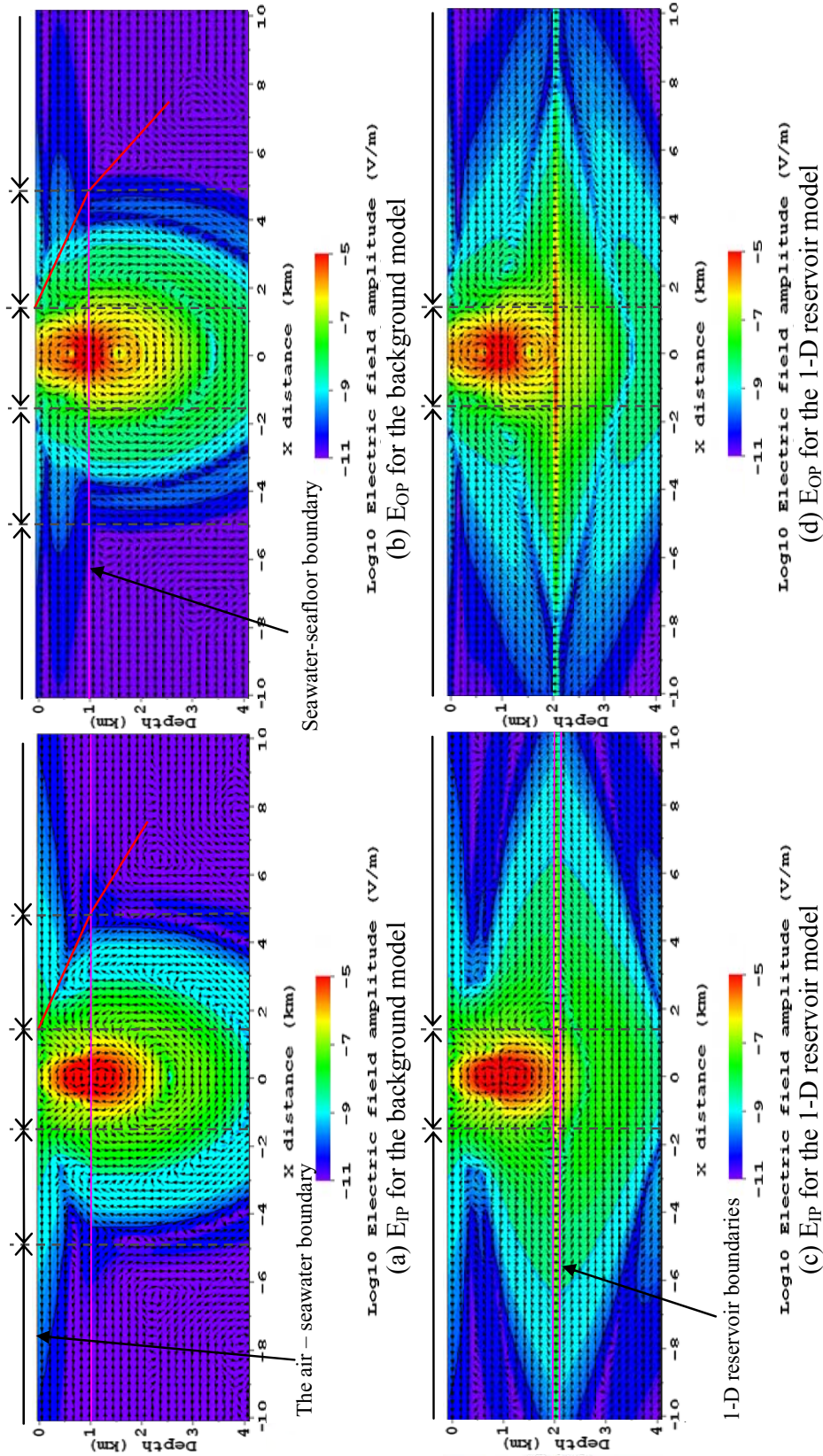


Figure 5.6. In-phase and out-of-phase E field distribution plots on the x-z plane at $y=0$ m for the background and 1-D reservoir models with a 0.63 Hz x-oriented HED source placed at (0 m, 0 m, 950 m). The same partition shown in Figure 5.5 is applied here.

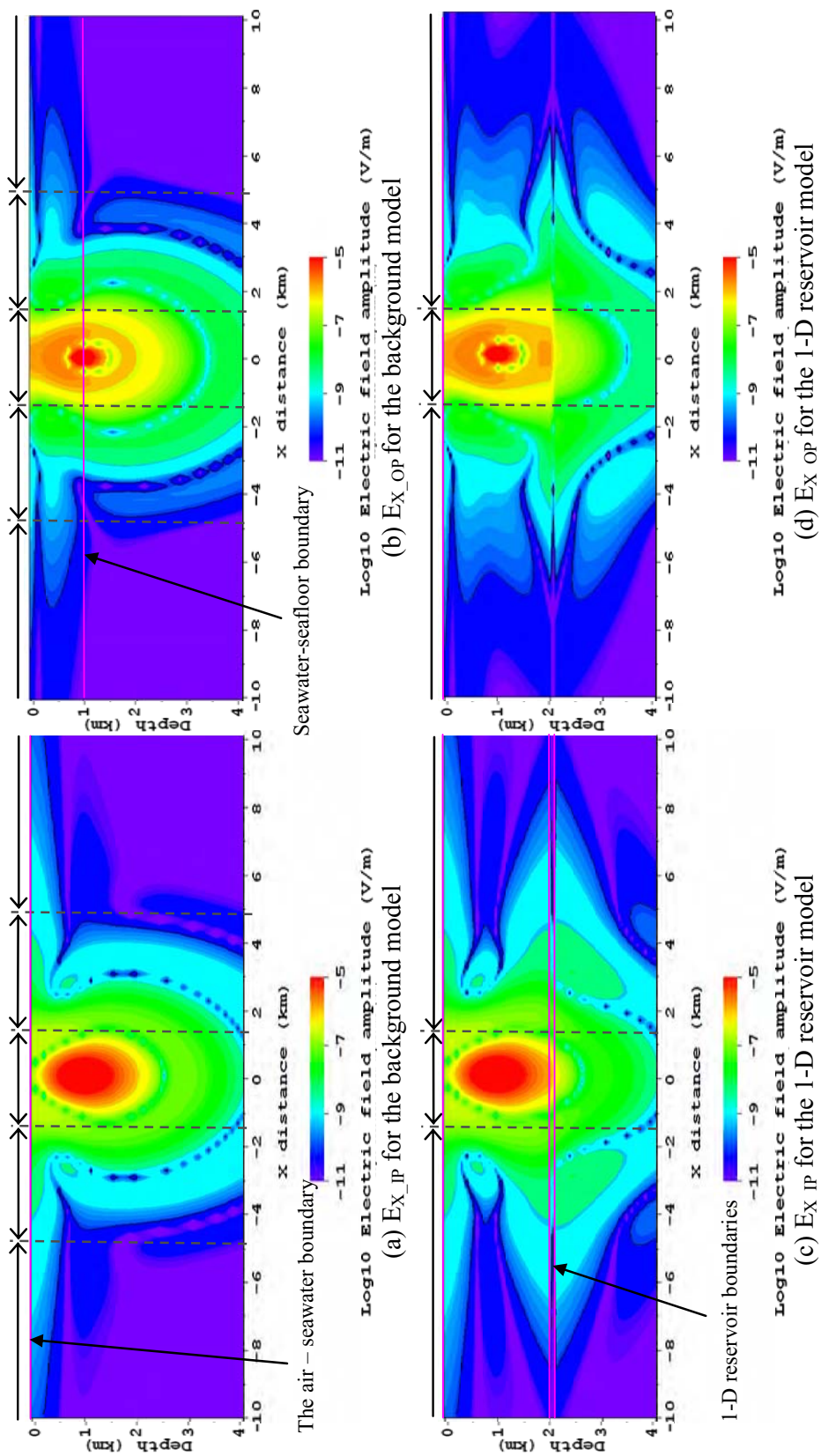


Figure 5.7. In-phase and out-of-phase E_X field distribution plots on the yz plane at $x=0$ m for the background and 1-D reservoir models with a 0.63 Hz x-oriented HED source placed at (0 m, 0 m, 950 m).

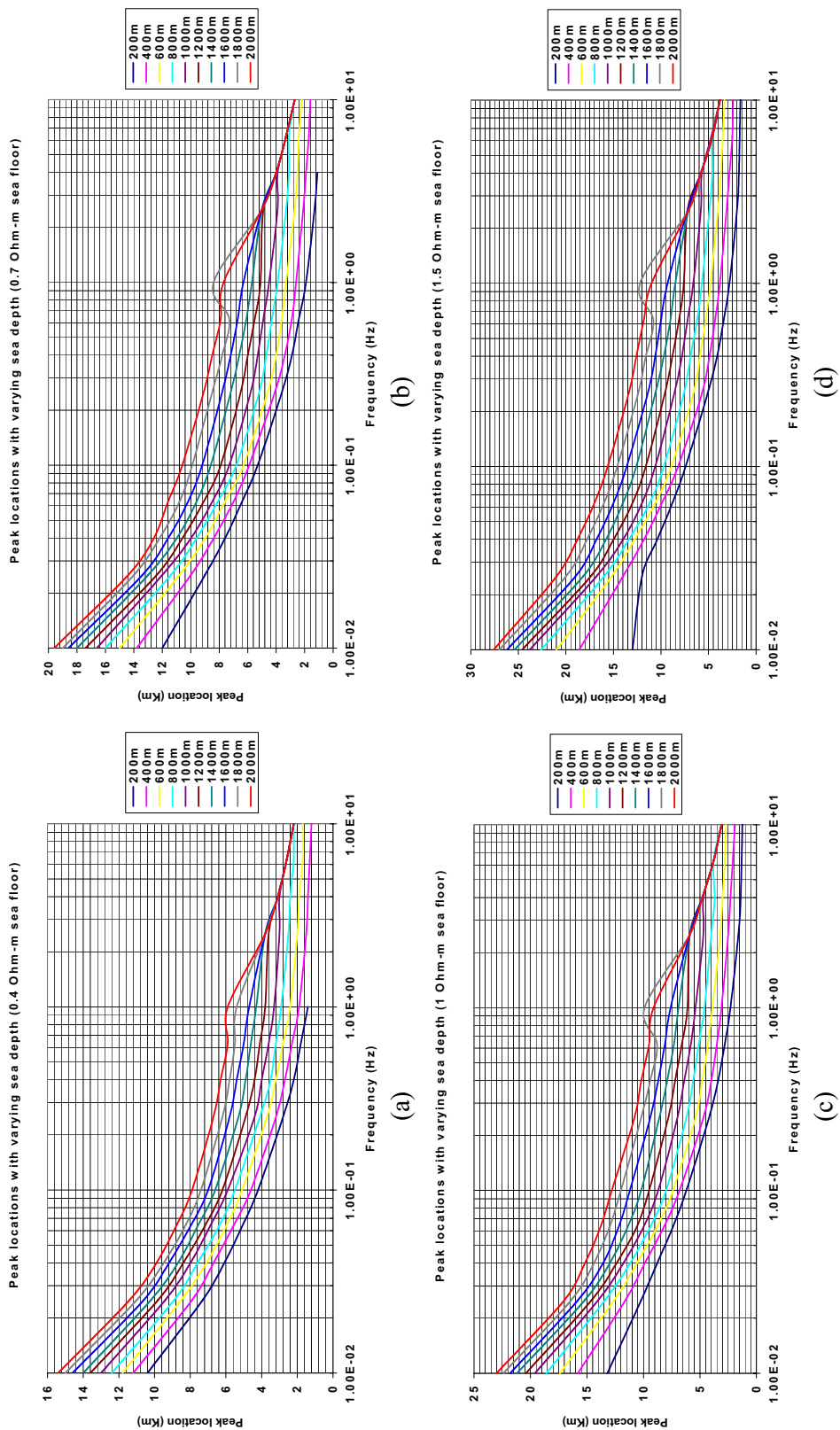
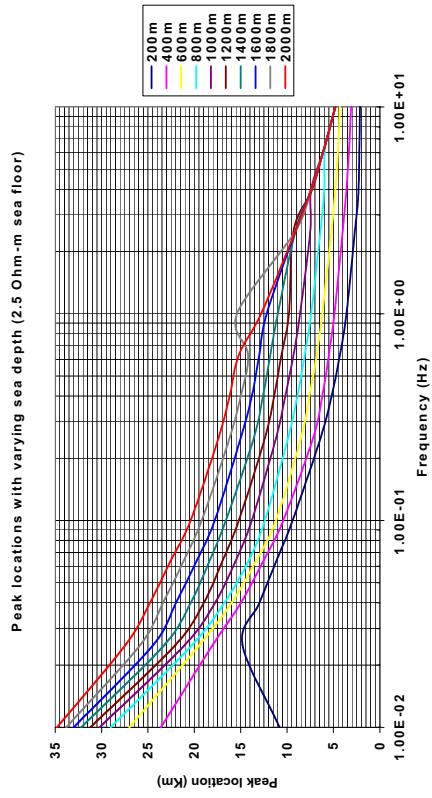
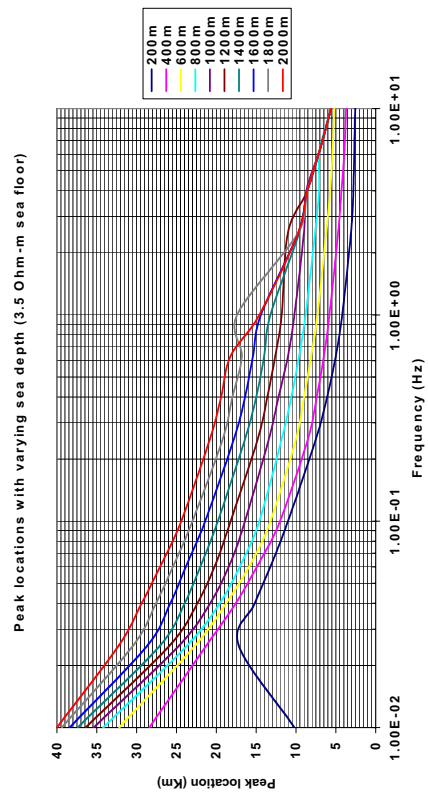


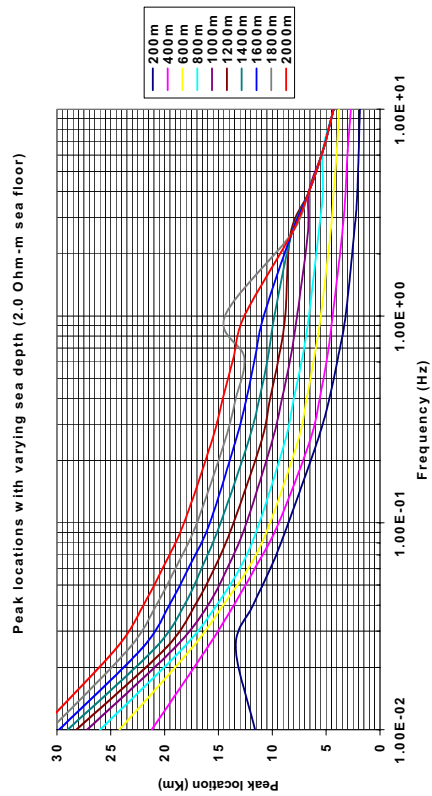
Figure 5.8. The distance from the source along the in-line survey line (in km) at which the normalized Ex peak occurs. An infinitesimal HED source is placed 50m above the seafloor and the resistivity of sea water was set to 0.3 Ohm-m.



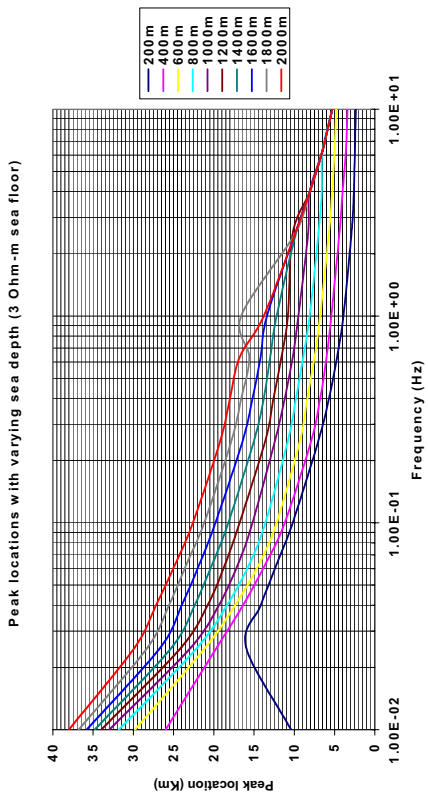
(f)



(h)



(e)



(g)

Figure 5.8. Continued.

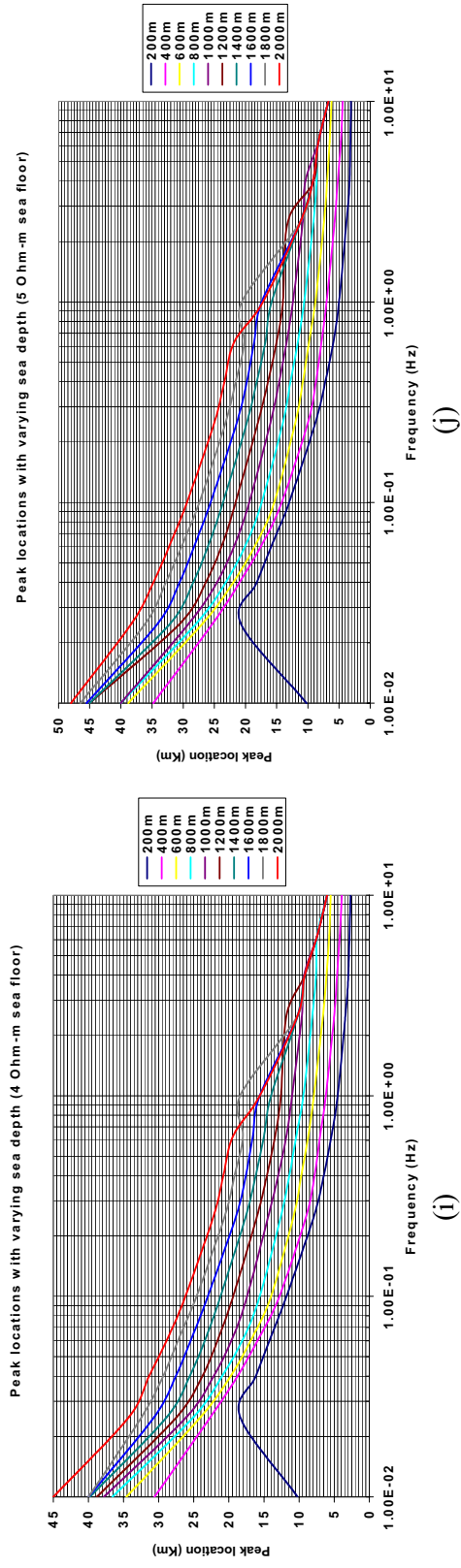


Figure 5.8. Continued.

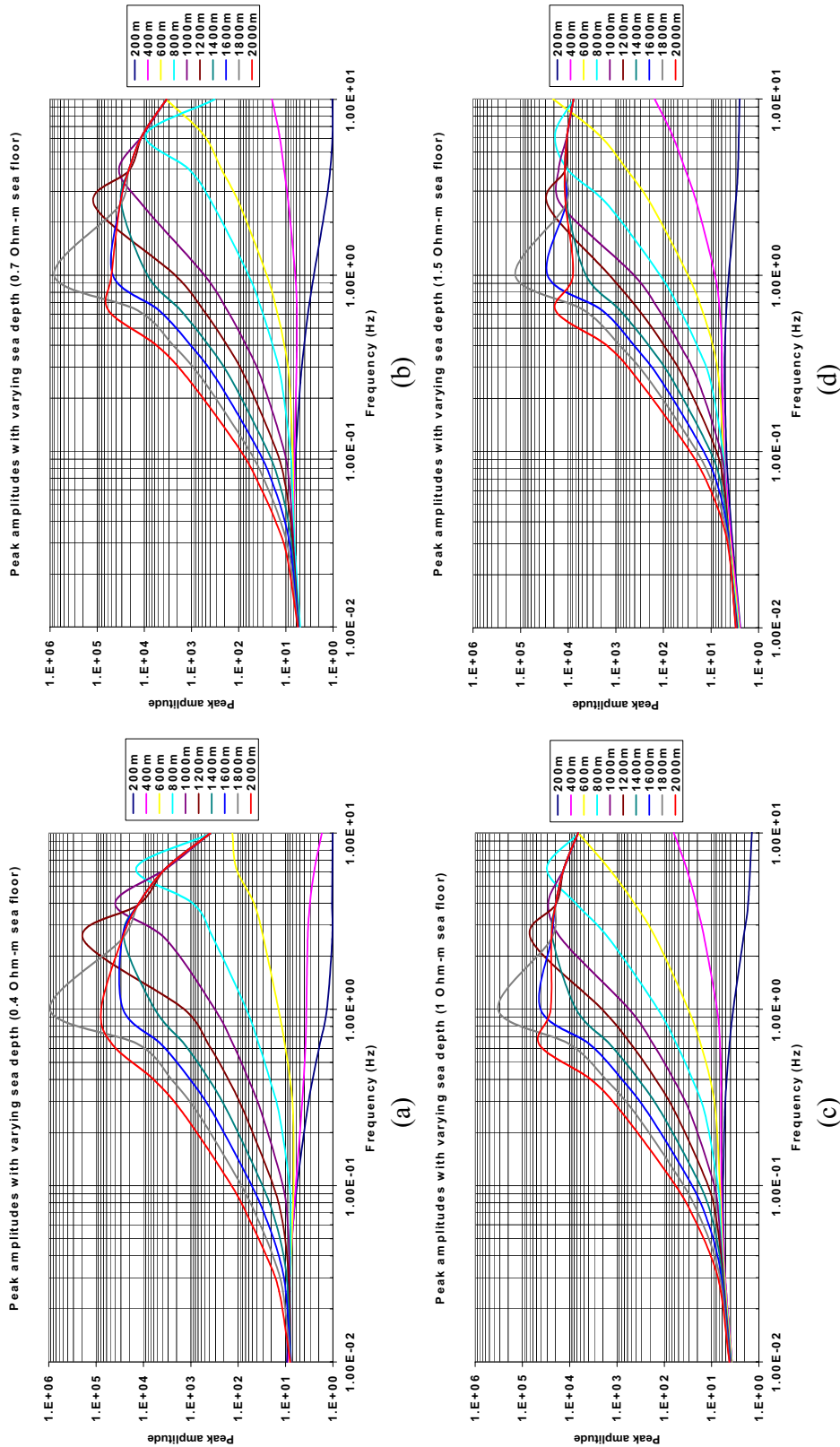


Figure 5.9. The peak amplitudes of normalized in-line Ex fields. The infinitesimal HED source is placed 50m above the seafloor and the resistivity of sea water was set to 0.3 Ohm-m.

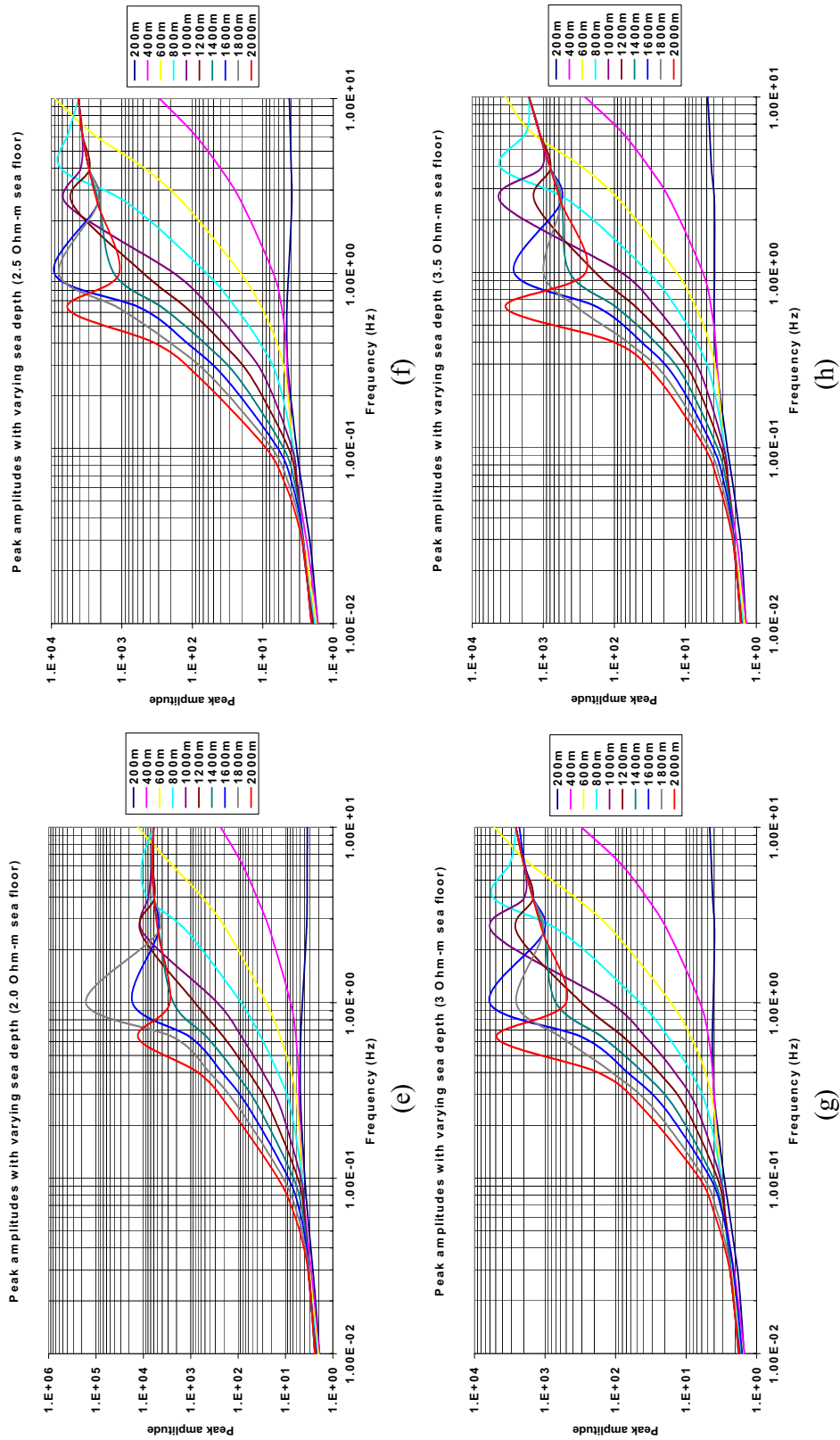


Figure 5.9. Continued.

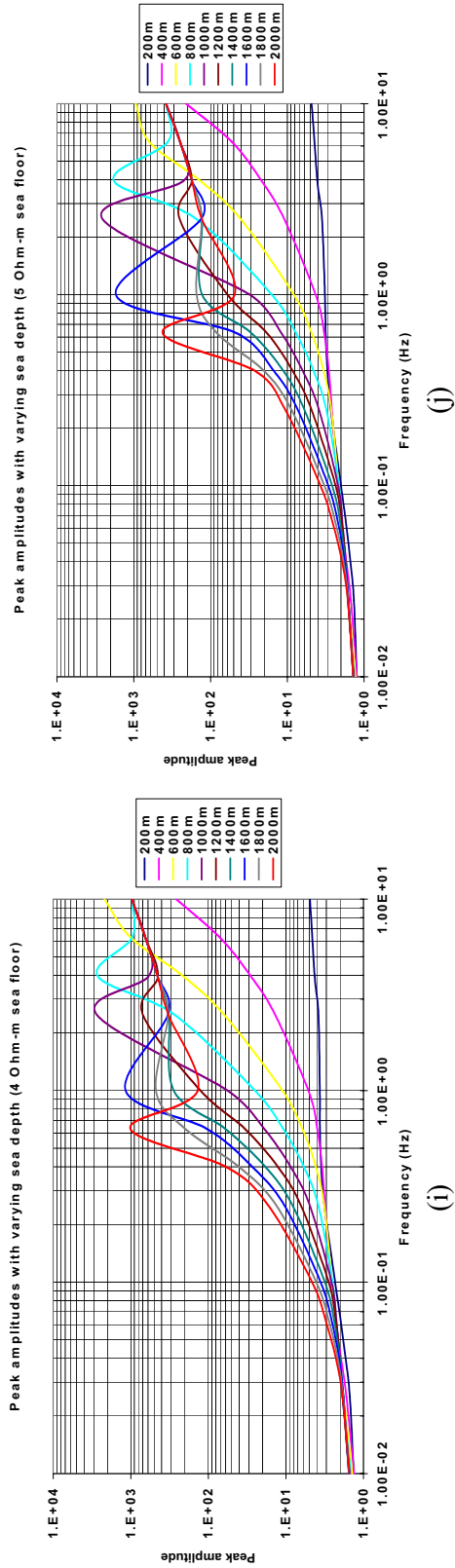


Figure 5.9. Continued.

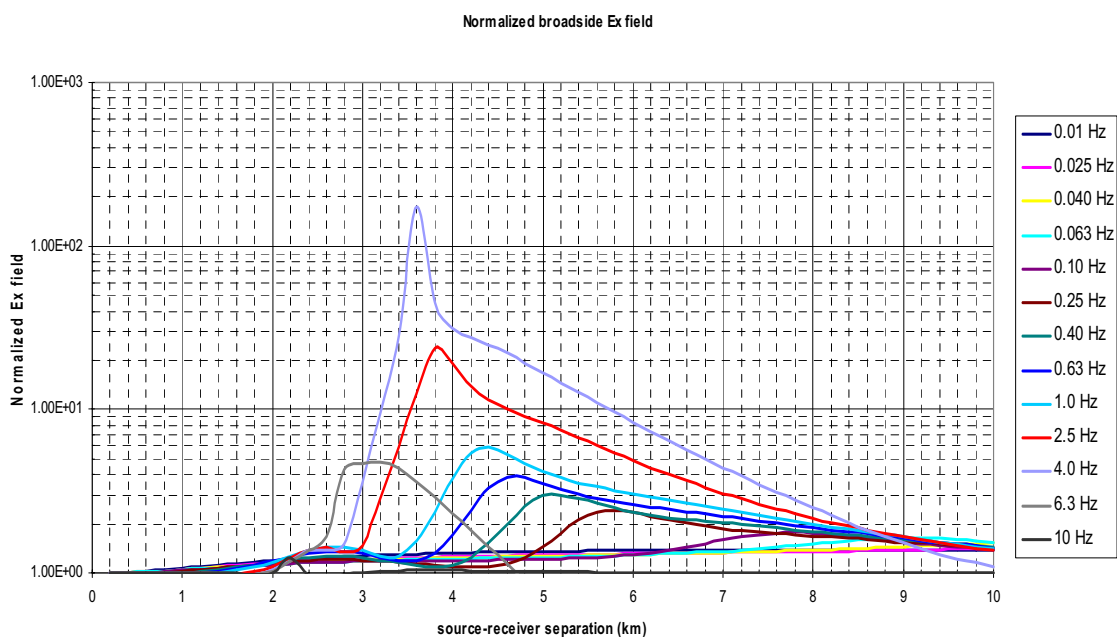
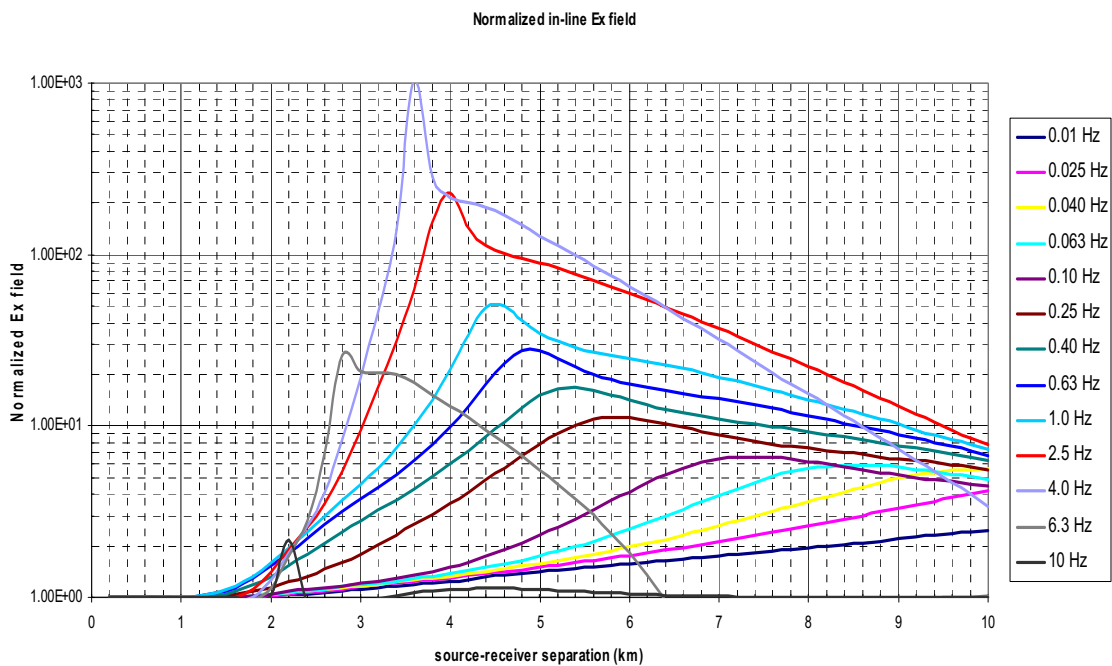


Figure 5.10. Normalized E_x responses at the frequencies ranging from $1.0E^{-2}$ Hz to 10 Hz. (a) the in-line E_x responses and (b) the broadside E_x responses.

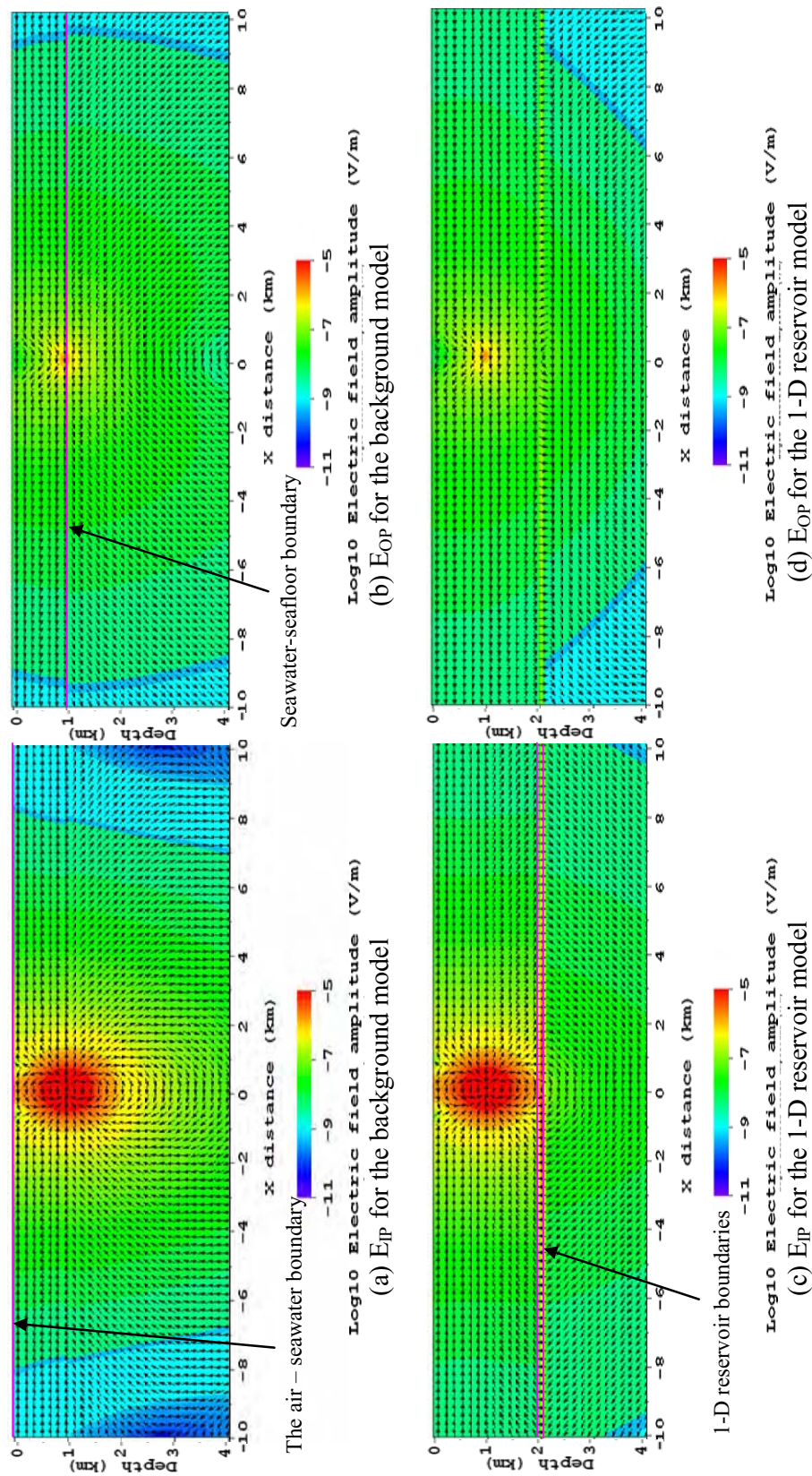


Figure 5.11. In-phase and out-of-phase electric field distribution plots on the xz cross-section at $y=0$ m for the background and 1-D reservoir models with a 0.01 Hz x-oriented HED source placed at (0 m, 0 m, 950 m).

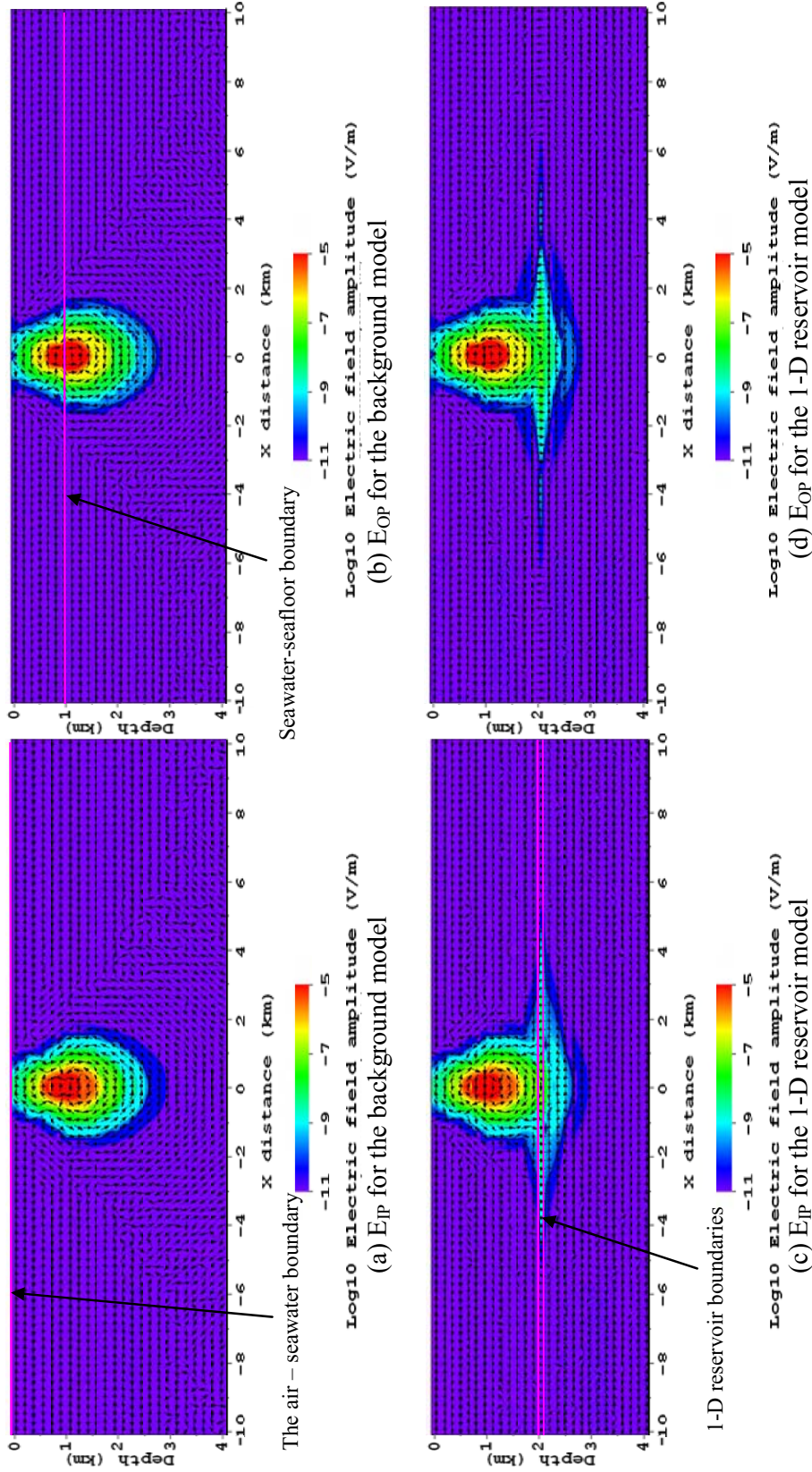
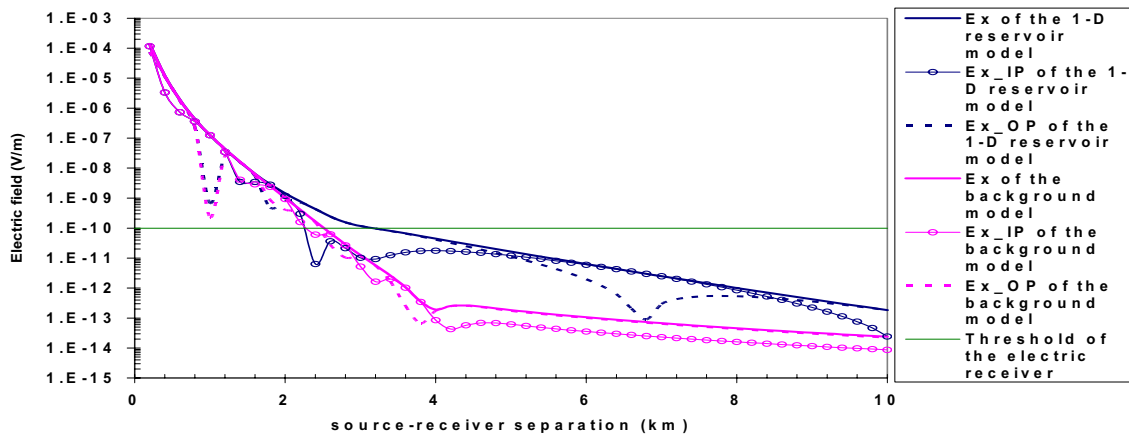
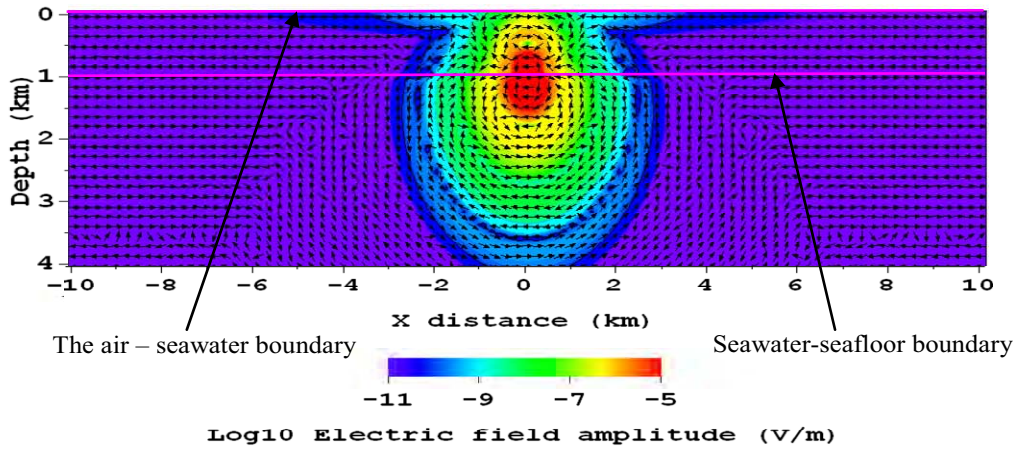


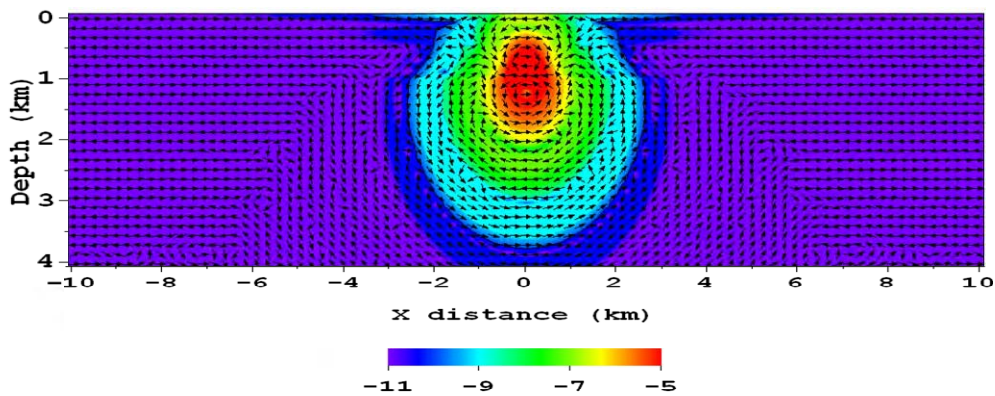
Figure 5.12. In-phase and out-of-phase electric field distribution plots on the xz cross-section at $y=0$ m for the background and 1-D reservoir models with a 10 Hz x-oriented HED source placed at (0 m, 0 m, 950 m).



(a) the in-line electric field responses



(b) E_{IP} for the background model



(c) E_{OP} for the background model

Figure 5.13. In-line E_x field responses and the cross-sectional views of electric field distribution with a 2.5 Hz x-oriented HED source.

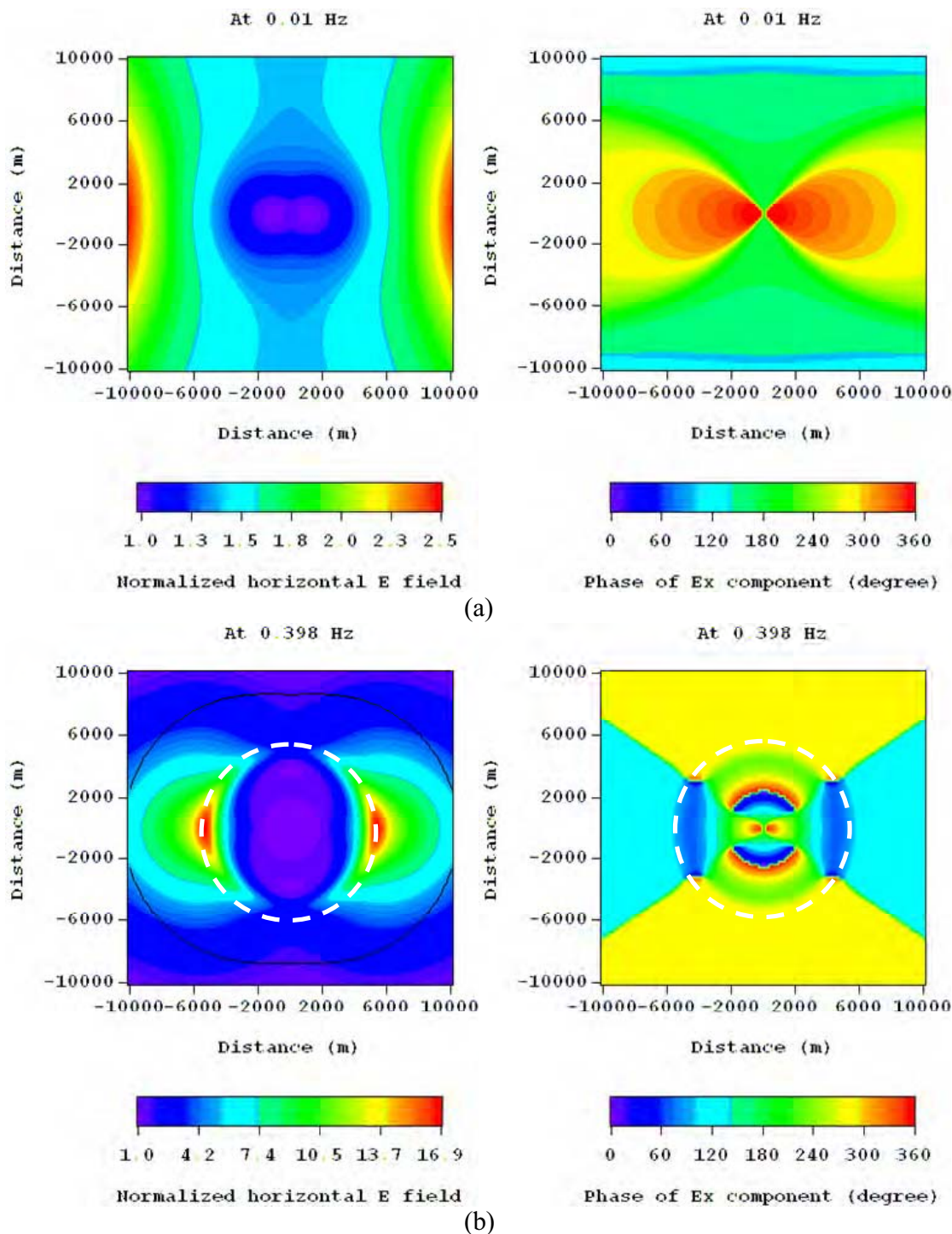


Figure 5.14. Normalized horizontal electric field plots (left column) for the 1-D reservoir model and E_x phase plots (right column) for the background model. The black contours represent the electric receiver noise level and the white ones represent the boundary beyond which the E_x phase becomes constant.

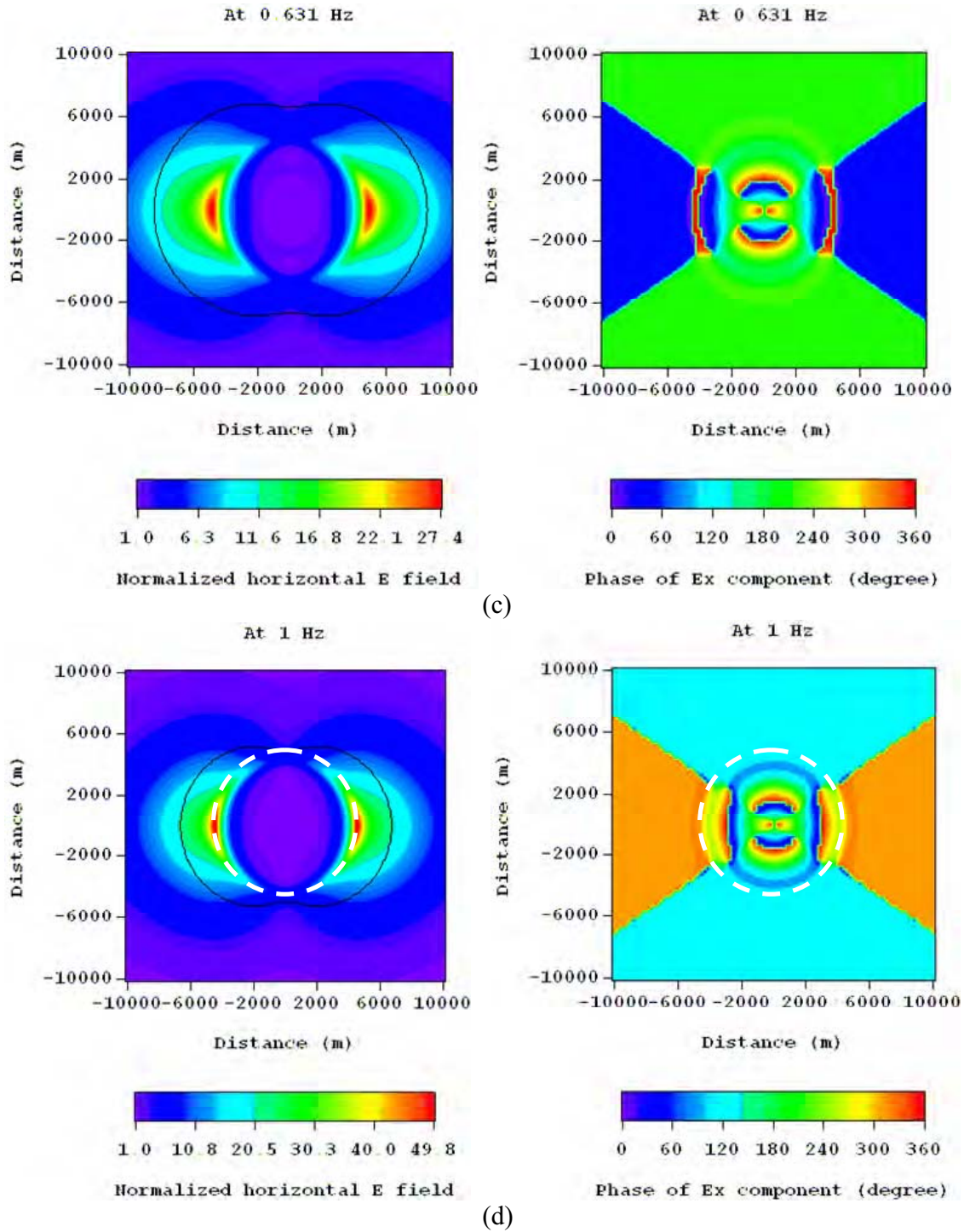
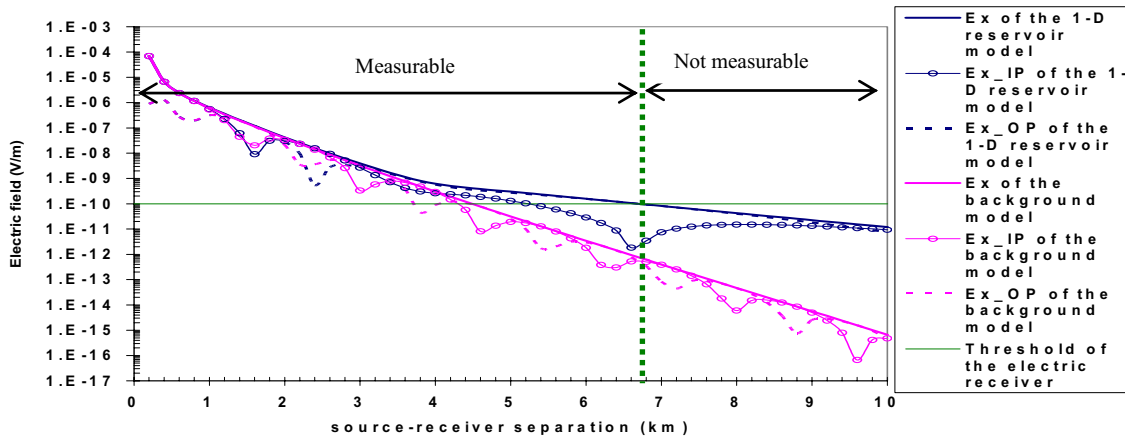
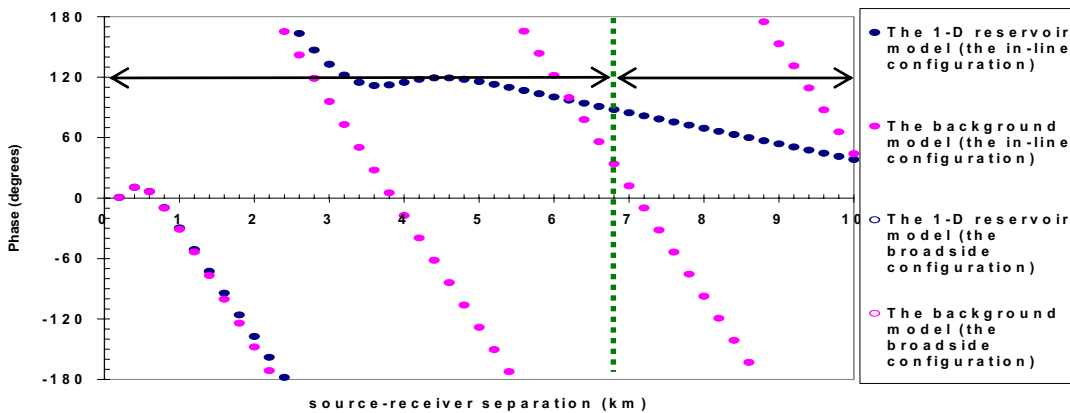


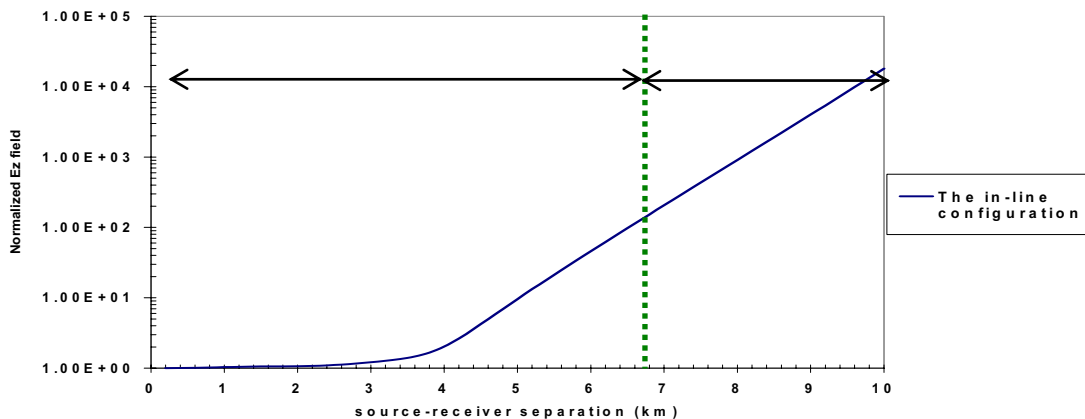
Figure 5.14. continued.



(a) The in-line E_z amplitudes



(b) The phases of the E_z components



(c) The normalized E_z response

Figure 5.15. In-line E_z responses with a 0.63 Hz x-oriented HED source for the background and 1-D reservoir models.

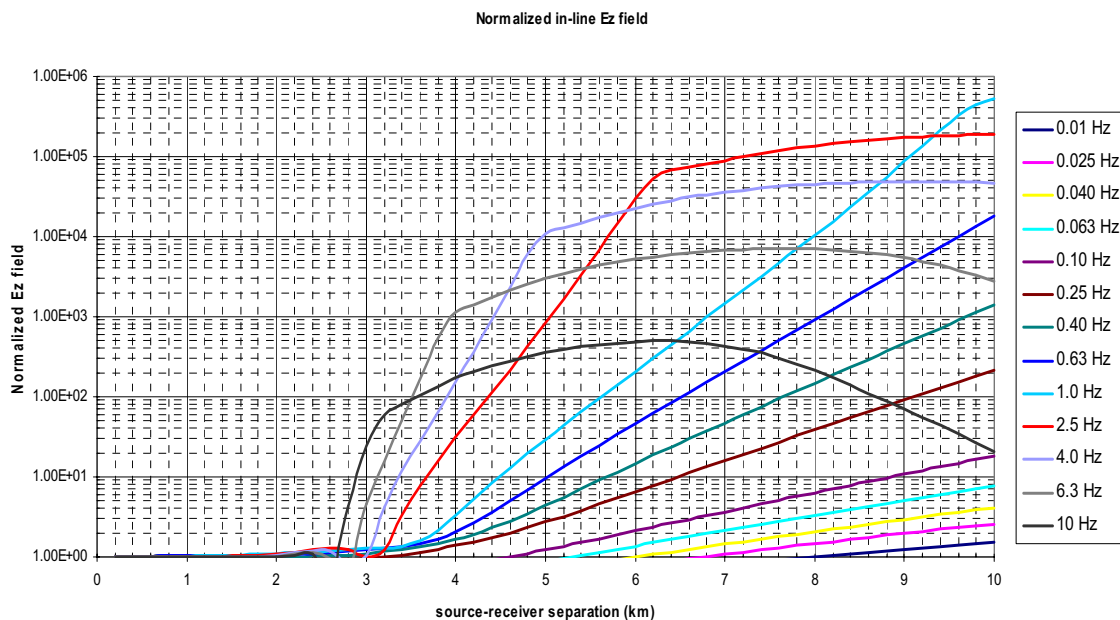


Figure 5.16. Normalized in-line E_z responses at the frequencies ranging from $1.0E^{-2}$ Hz to 10 Hz.

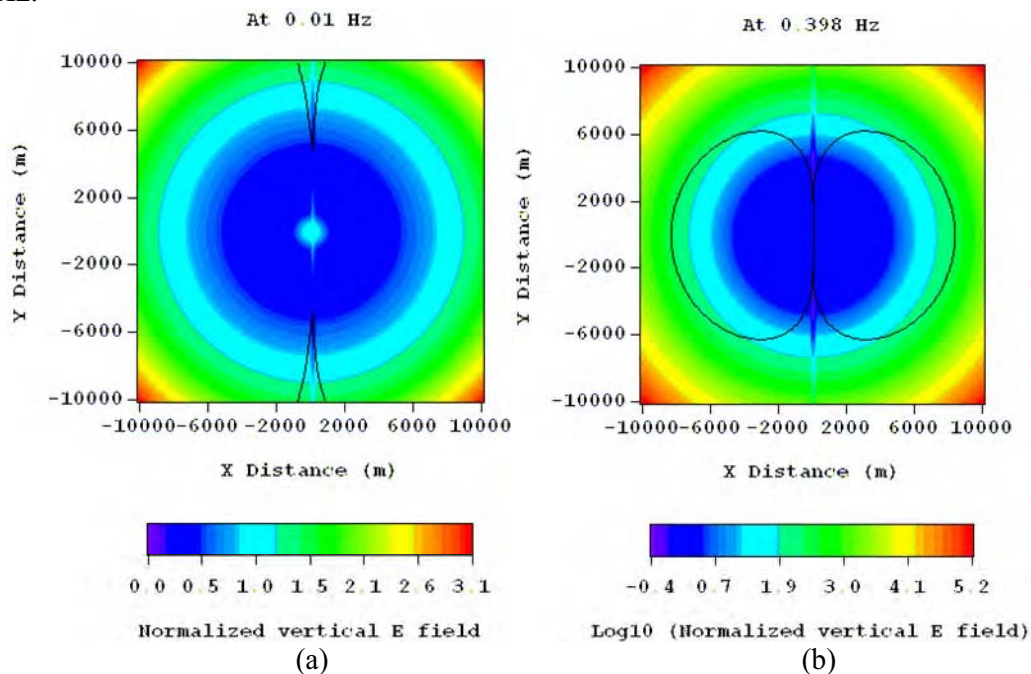


Figure 5.17. Normalized vertical electric field responses for the 1-D reservoir model. (a) has the linear scale color chart and others the log scale color chart. Black contours represent the electric receiver noise level.

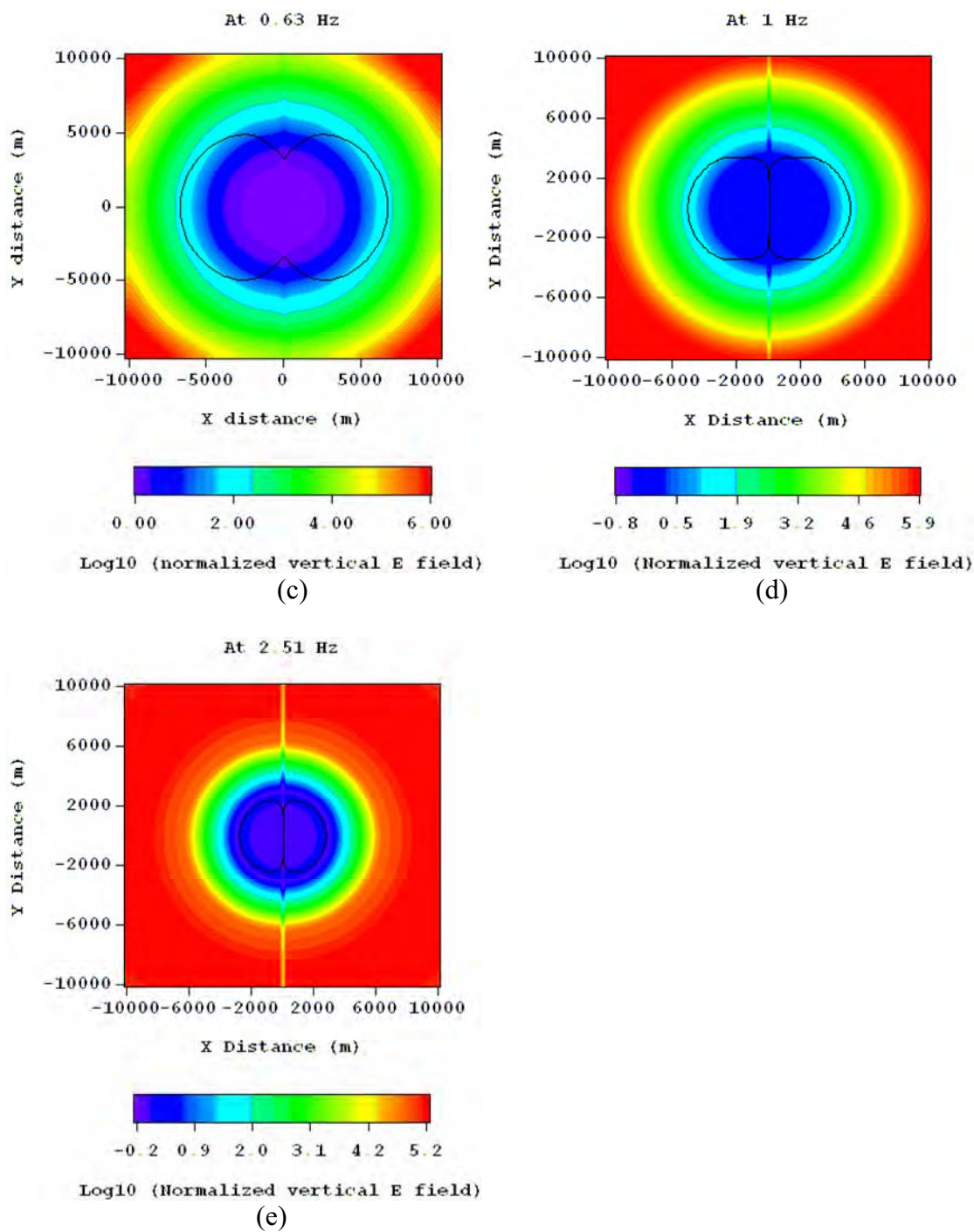


Figure 5.17. Continued.

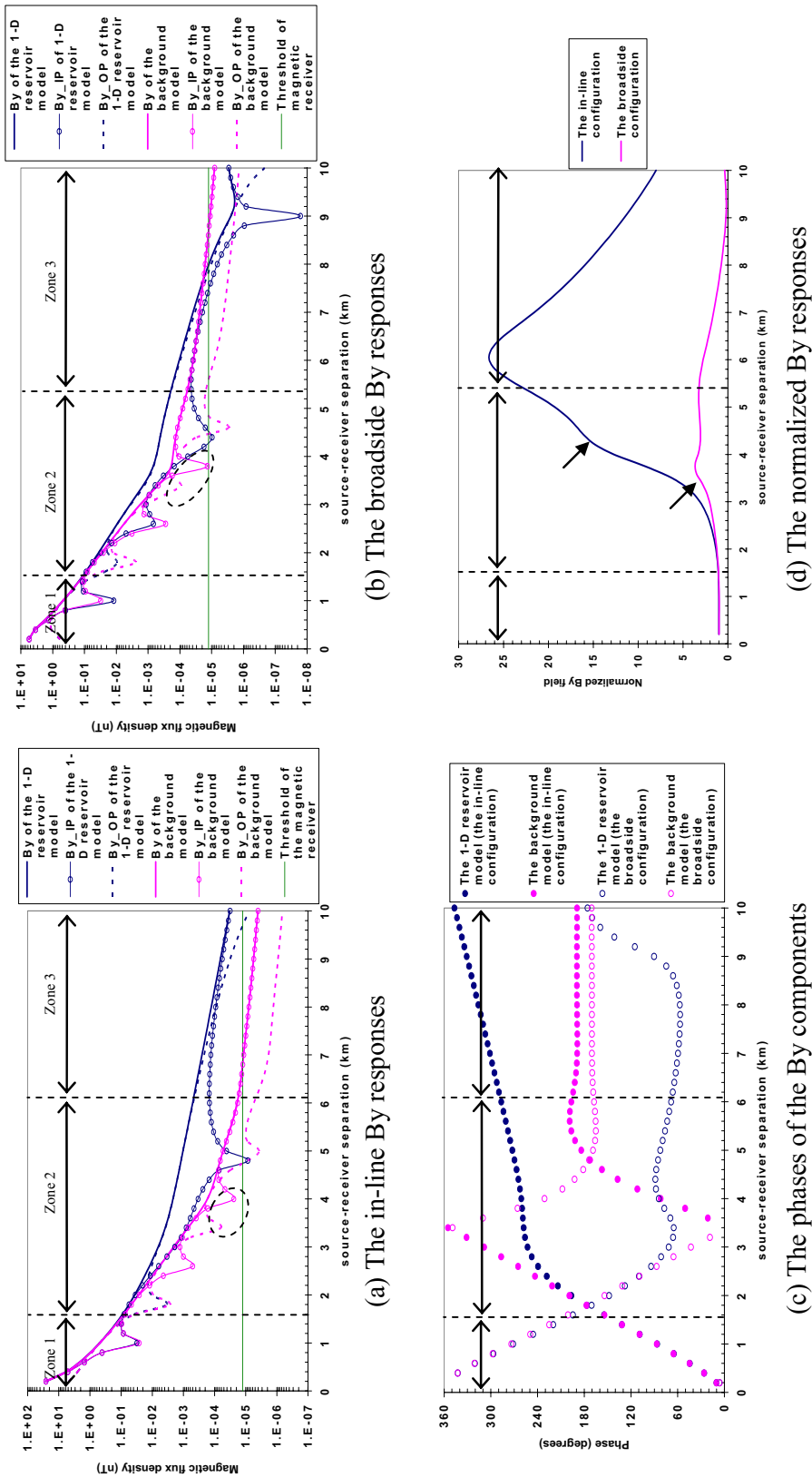


Figure 5.18. B_Y responses with a 0.63 Hz x-oriented HED source for the background and 1-D reservoir models. The partition of the left plots are based on the in-line responses and that of the right ones the broadside responses. The arrows in (d) indicate the secondary peaks.

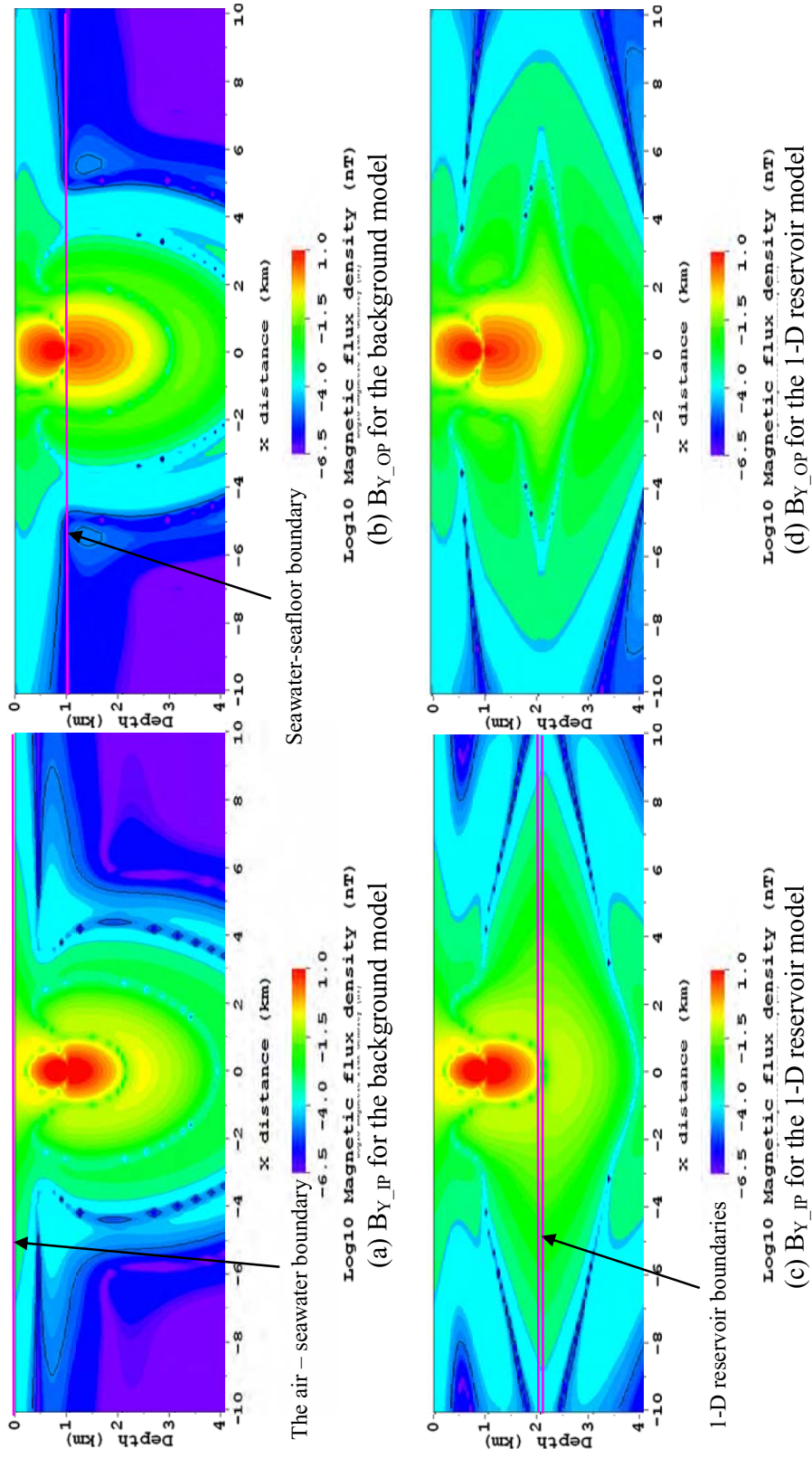


Figure 5.19. In-phase and out-of-phase B_Y distribution plots on the xz cross-section at $y=0$ m for the background and 1-D reservoir models with a 0.63 Hz x-oriented HED source placed at (0 m, 0 m, 950 m).

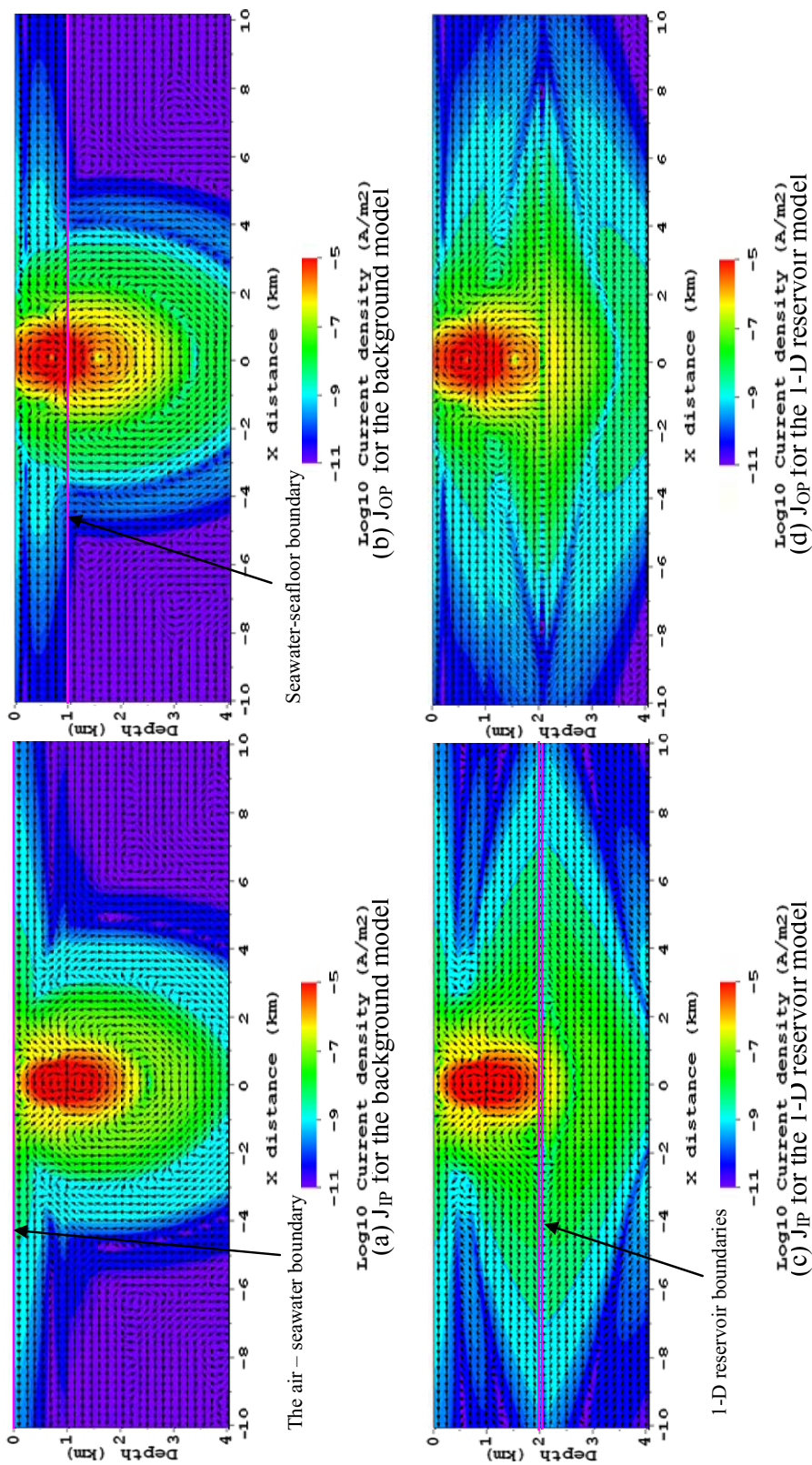


Figure 5.20. In-phase and out-of-phase current distribution plots on the xz cross-section at $y=0$ m for the background and 1-D reservoir models with a 0.63 Hz x-oriented HED placed at (0 m, 0 m, 950 m).

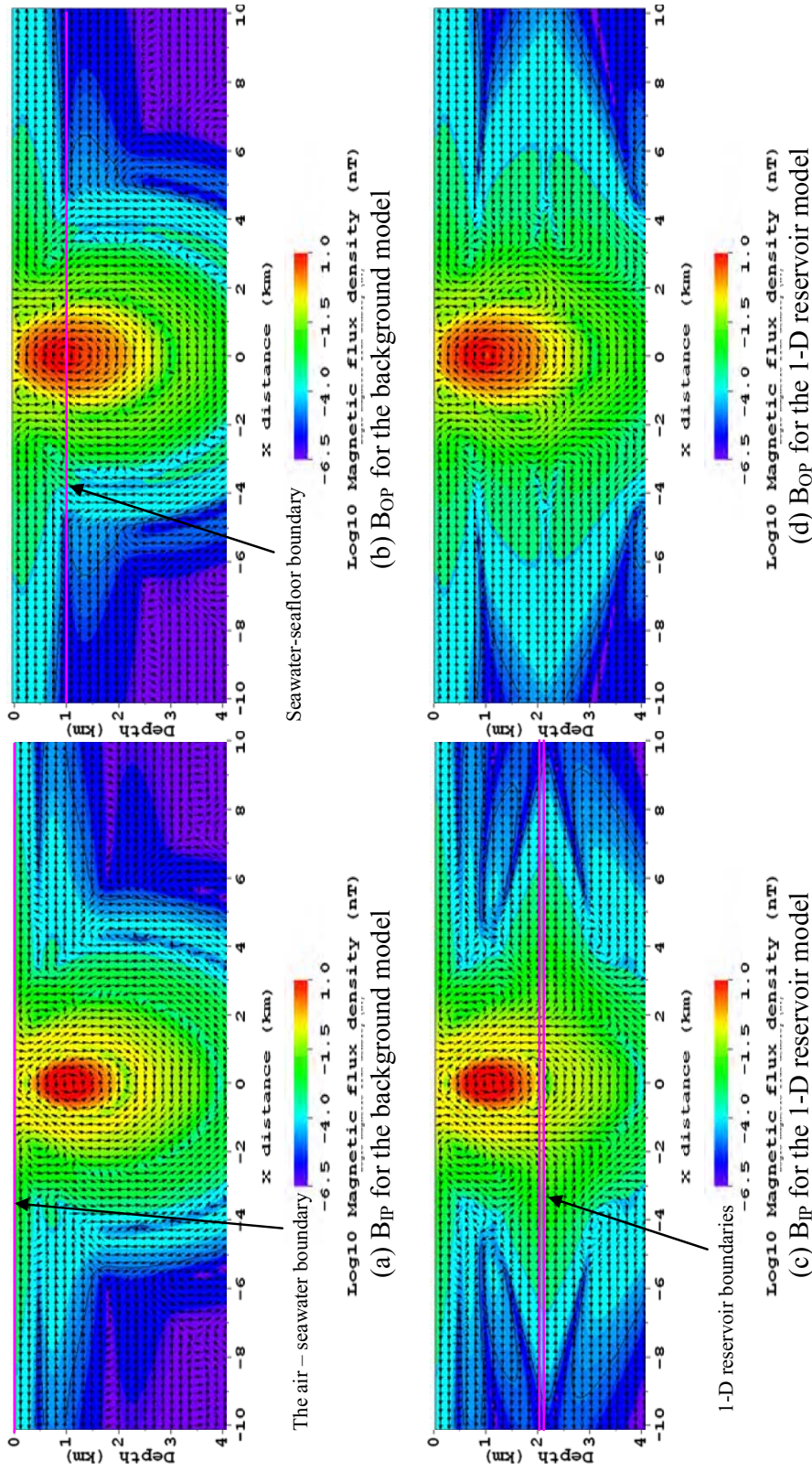


Figure 5.21. In-phase and out-of-phase B distribution plots on the yz cross-section at x=0 m for the background and 1-D reservoir models with a 0.63 Hz x-oriented HED source placed at (0 m, 0 m, 950 m).

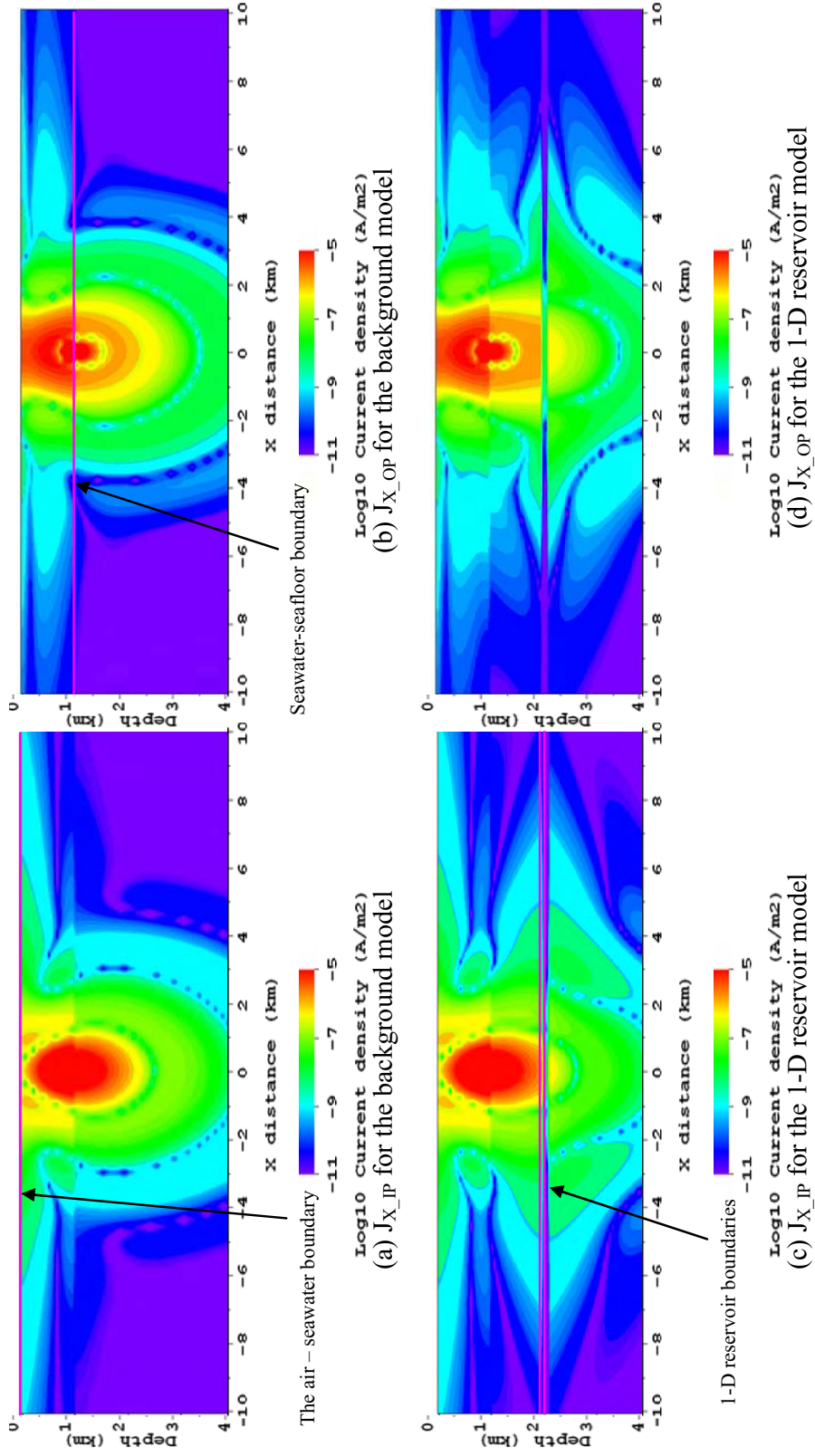


Figure 5.22. In-phase and out-of-phase J_x amplitude distribution plots on the yz cross-section at $x=0$ m for the background and the 1-D reservoir models with a 0.63 Hz x-oriented HED source placed at (0 m, 0 m, 950 m).

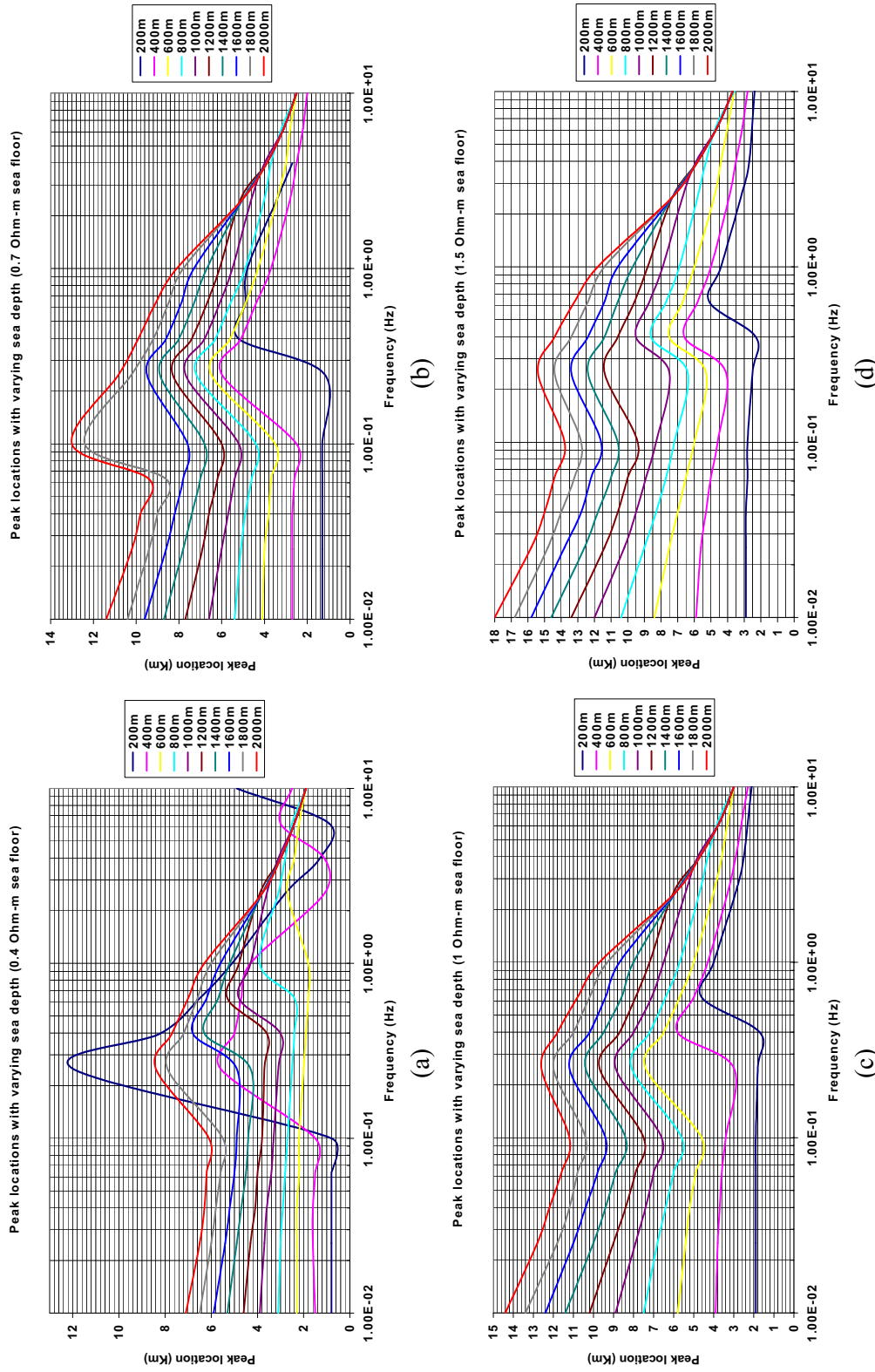


Figure 5.23. The distance from the source along the in-line survey line (in km) at which the normalized B_y peak occurs. An infinitesimal HED source is placed 50m above the seafloor and the resistivity of sea water was set to 0.3 Ohm-m.

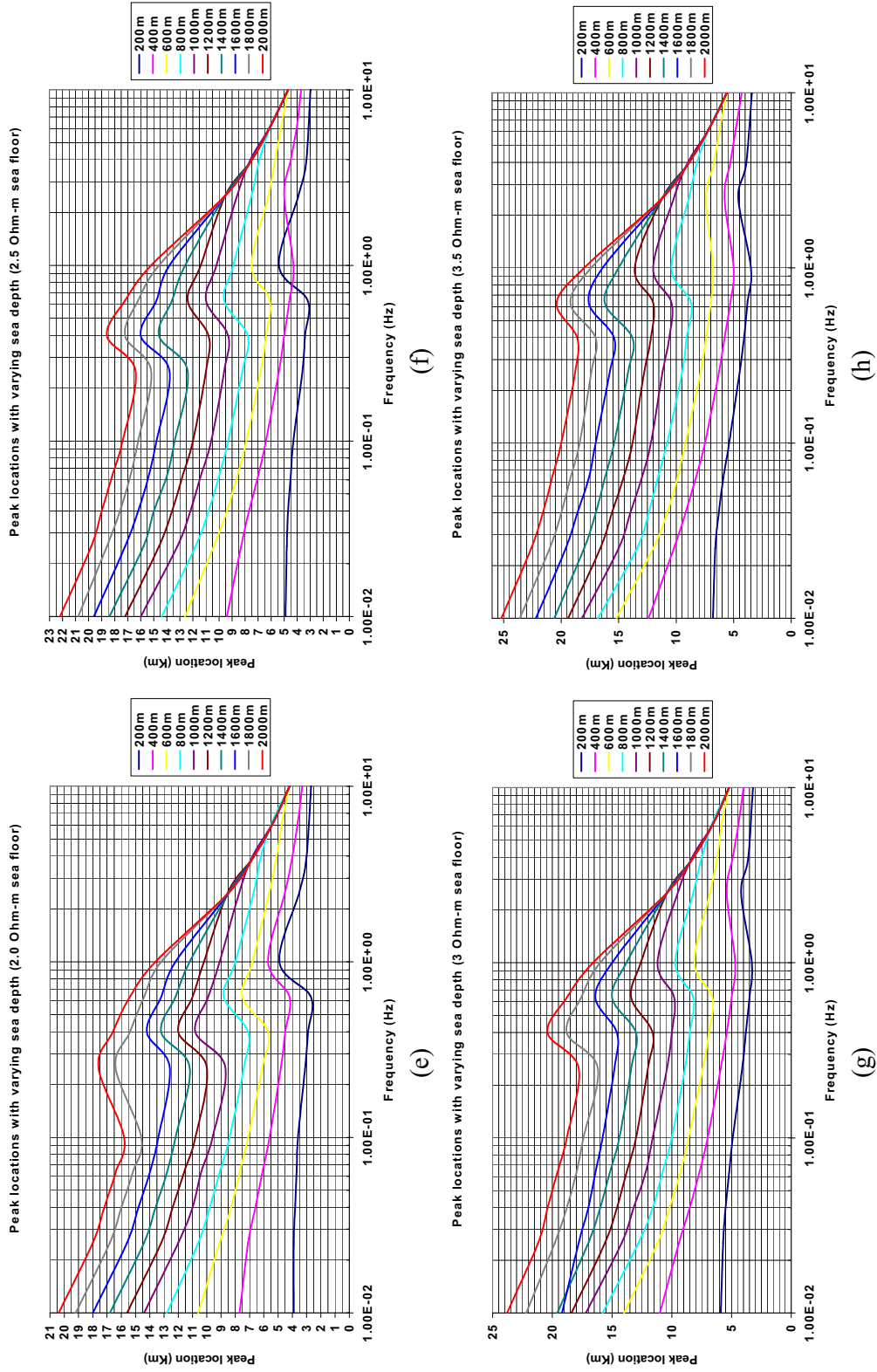


Figure 5.23. Continued.

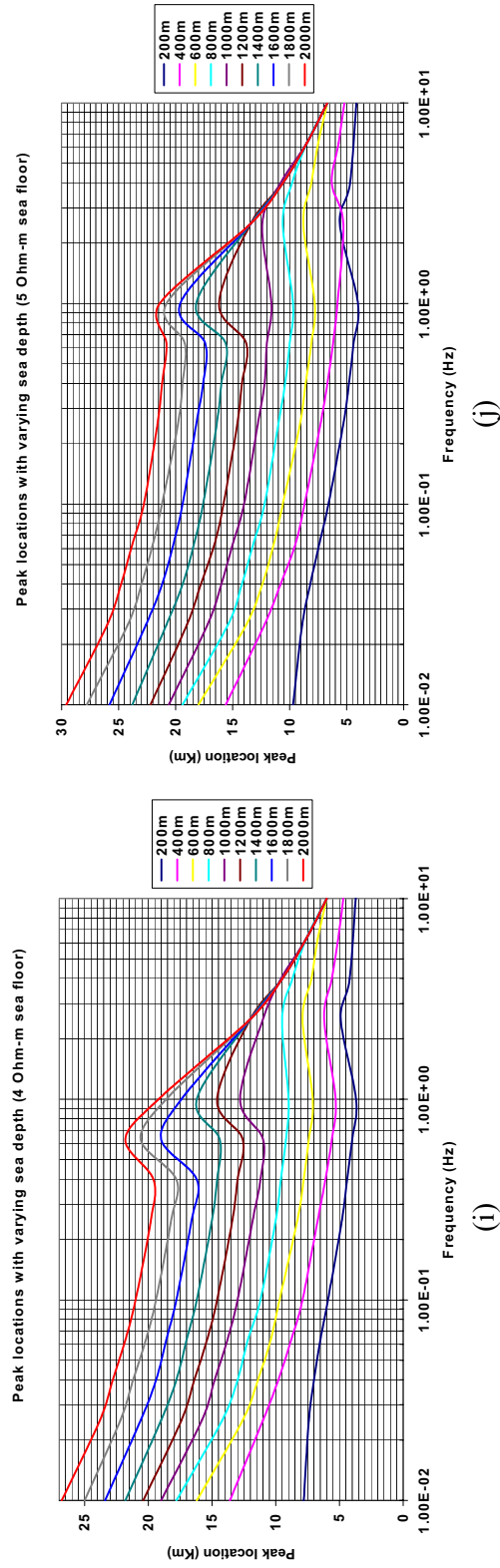


Figure 5.23. Continued.

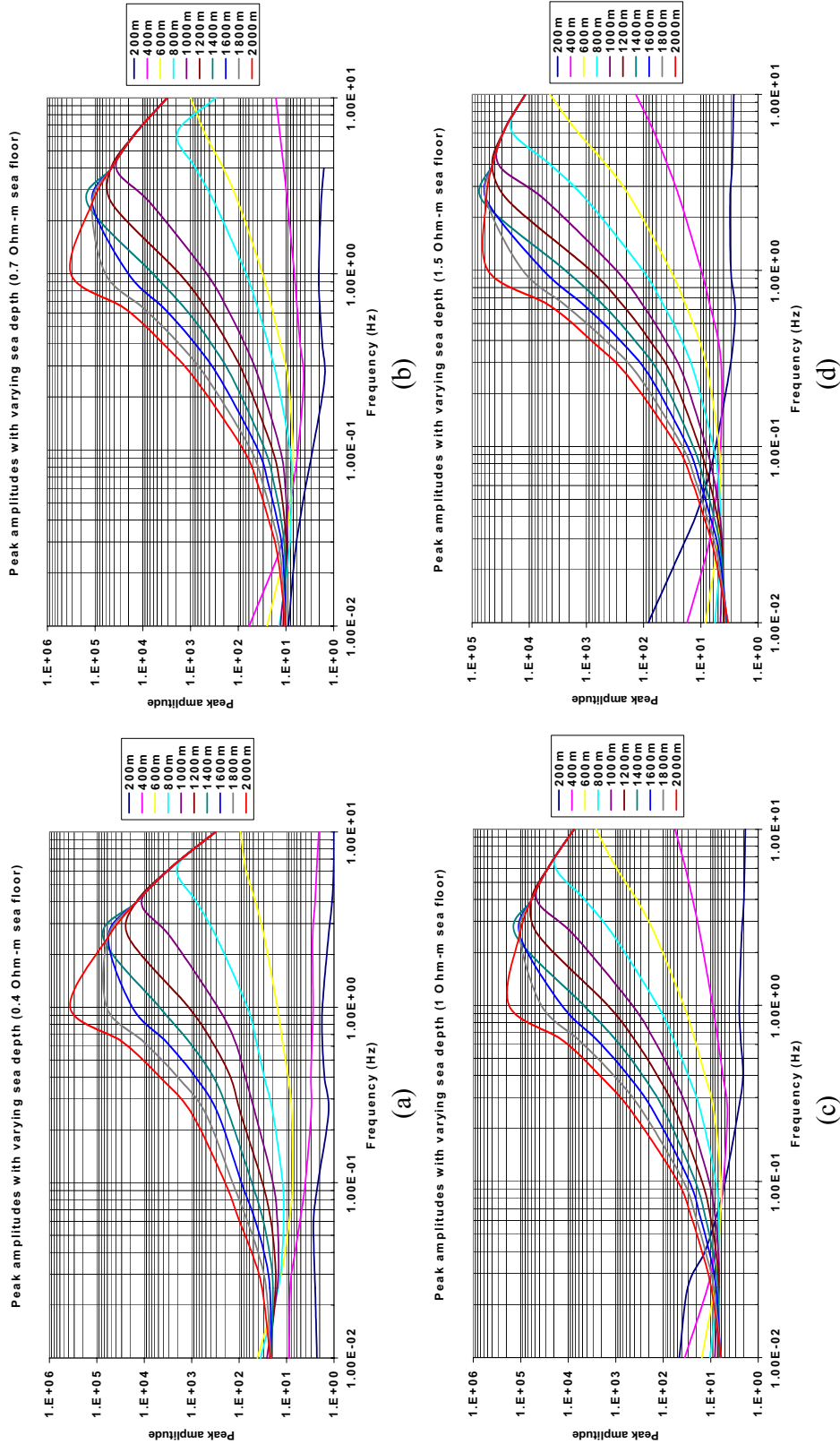
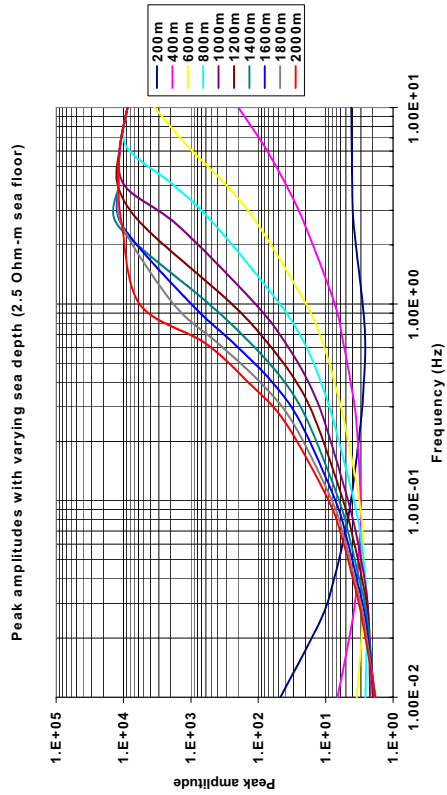
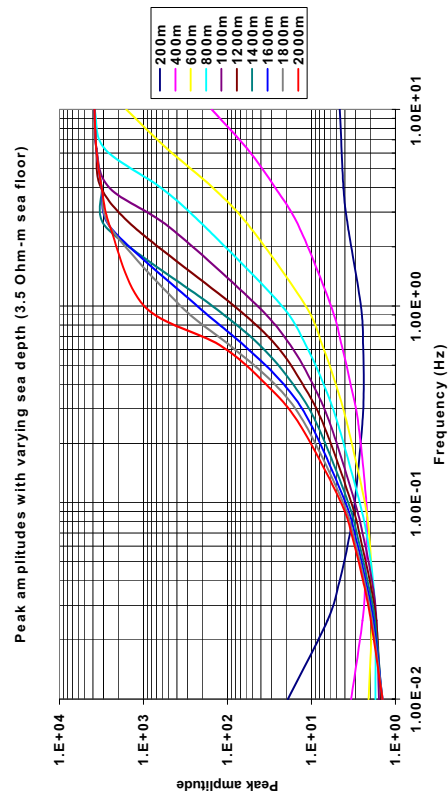


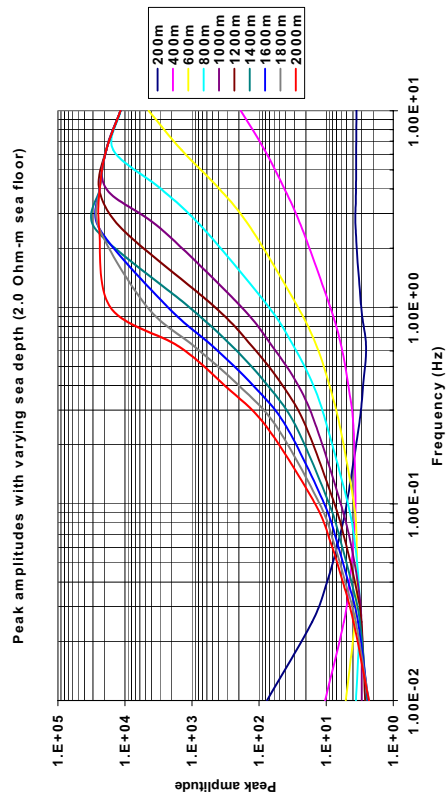
Figure 5.24. The peak amplitudes of normalized B_y field for the in-line configuration. An infinitesimal HED is placed 50m above the seafloor and the resistivity of seawater was set to 0.3 Ohm-m.



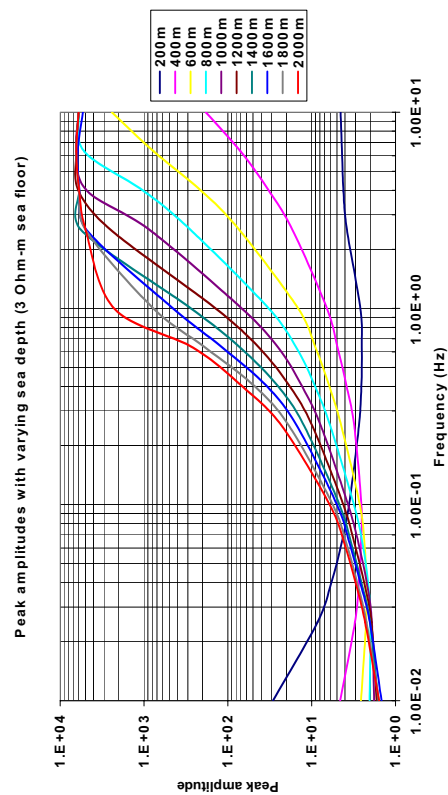
(f)



(h)



(e)



(g)

Figure 5.24. Continued.

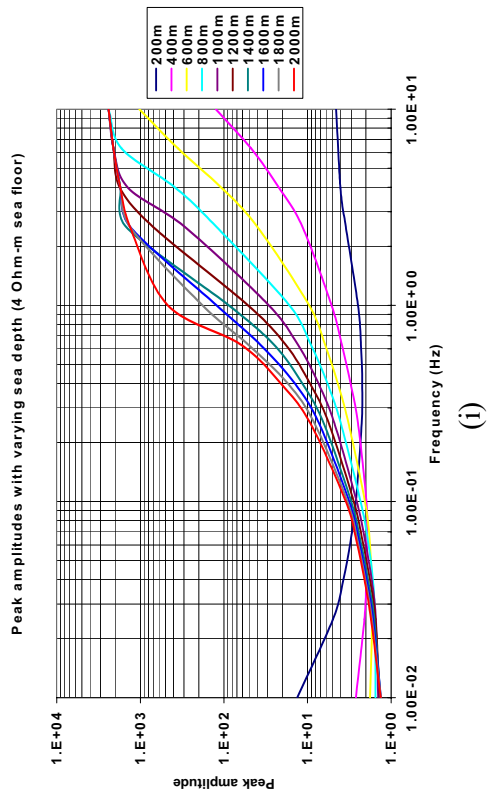
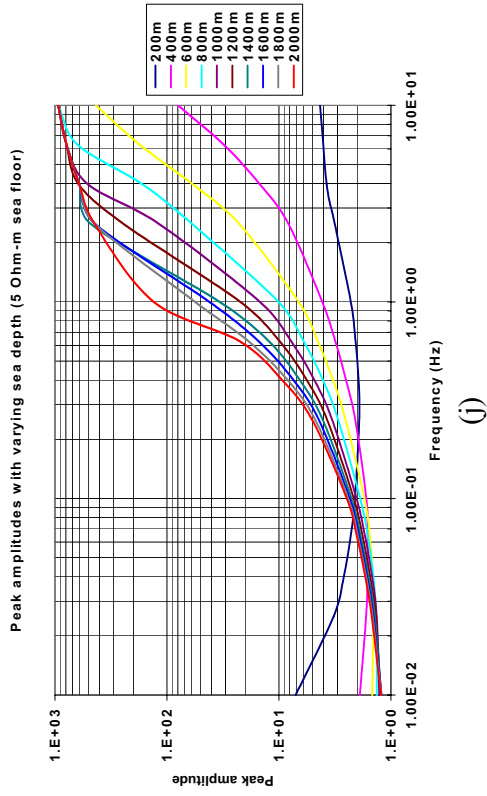


Figure 5.24. Continued.

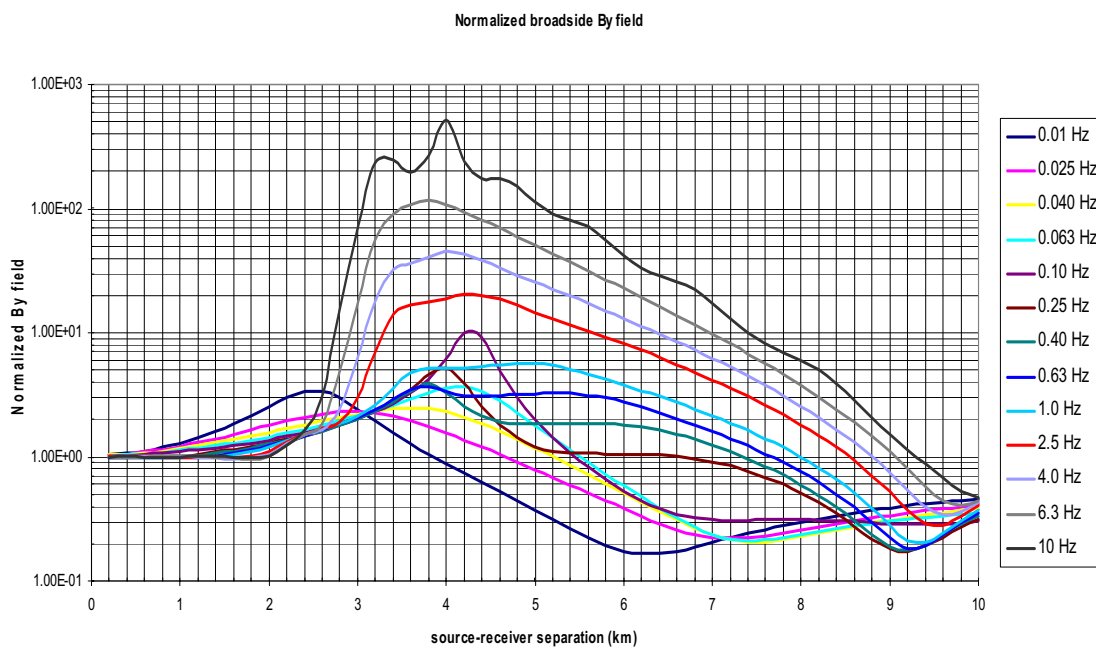
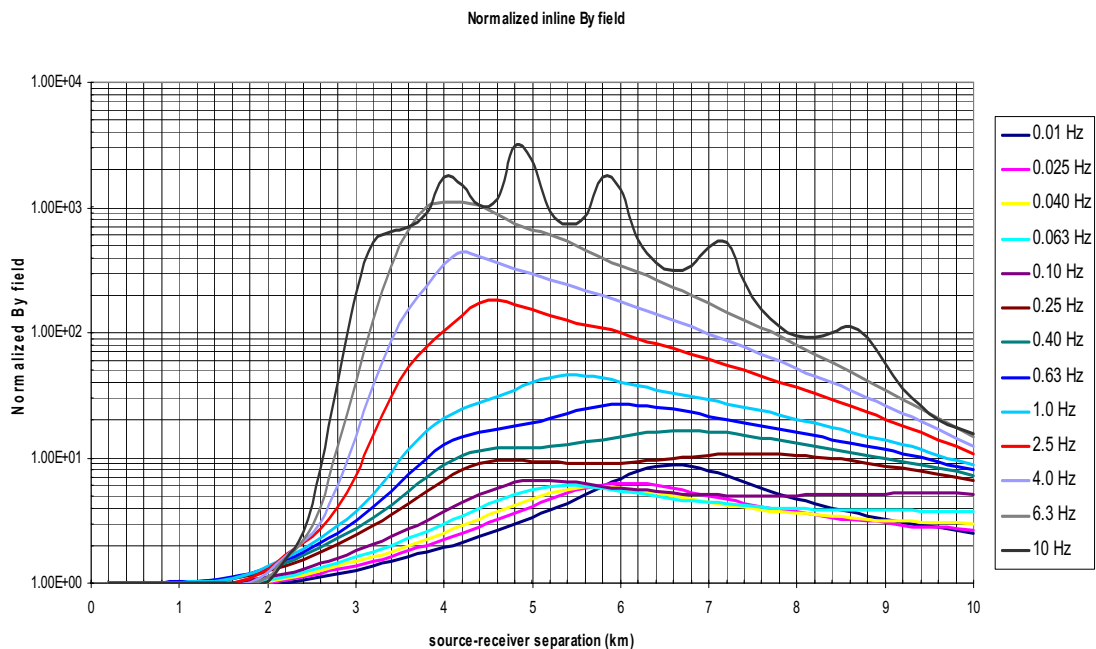


Figure 5.25. Normalized B_y responses at the frequencies ranging from $1.0E^{-2}$ Hz to 10 Hz. (a) the in-line responses and (b) the broadside responses.

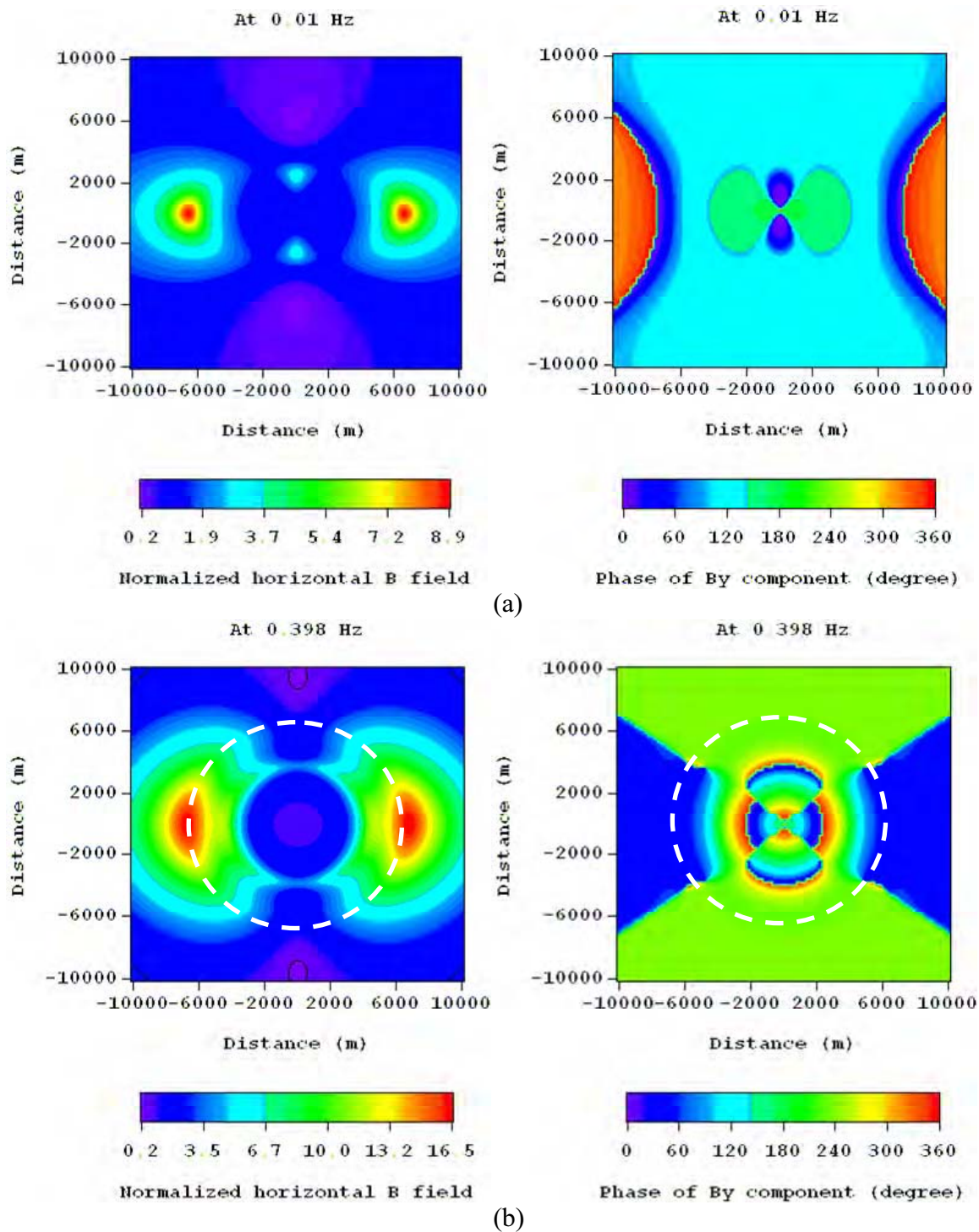


Figure 5.26. Normalized horizontal magnetic responses (left column) for the 1-D reservoir model, and B_Y phase plots (right column) for the background model. The black contours represent magnetic noise level and the white ones represent the boundary beyond which the B_Y phase becomes constant.

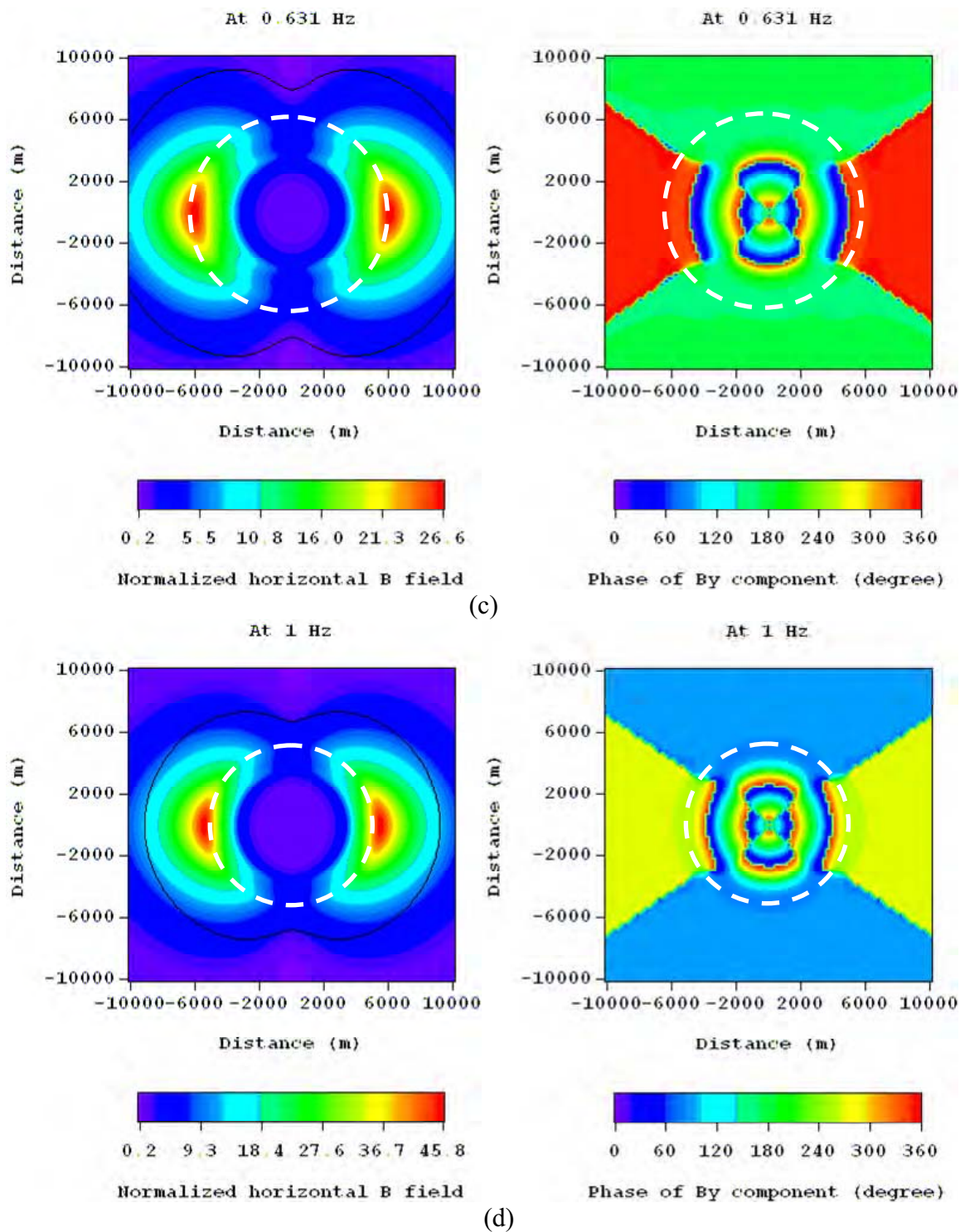


Figure 5.26. Continued.

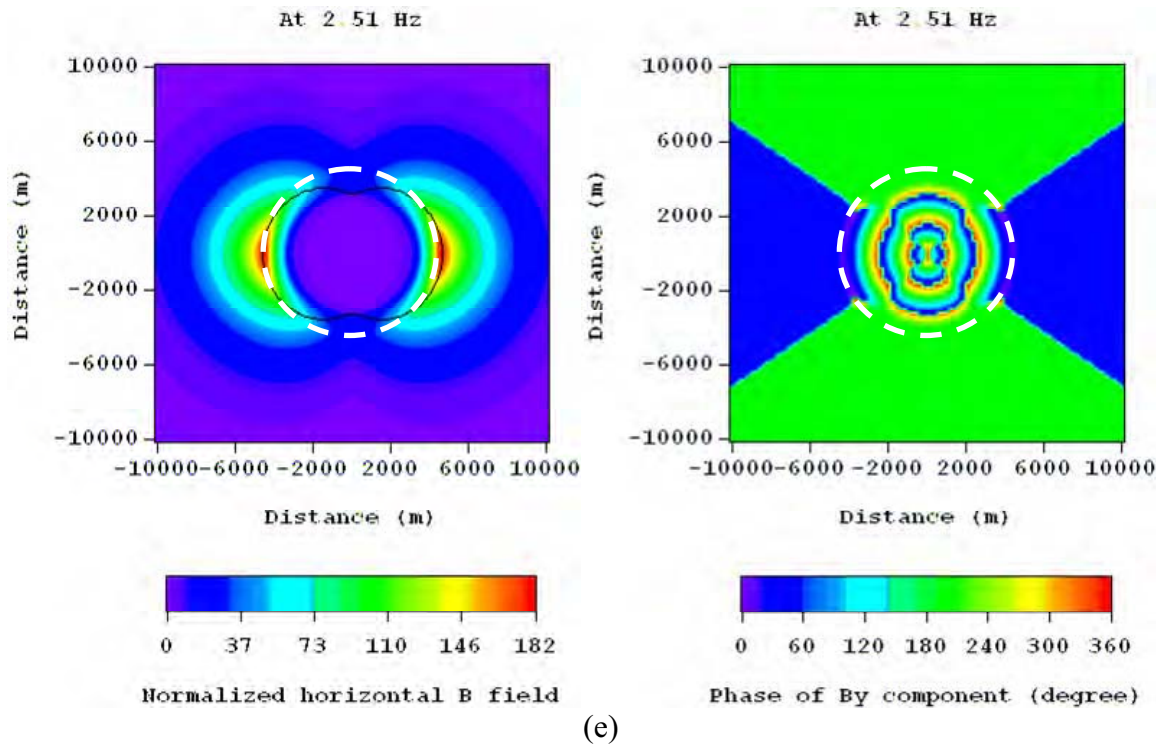


Figure 5.26. Continued.

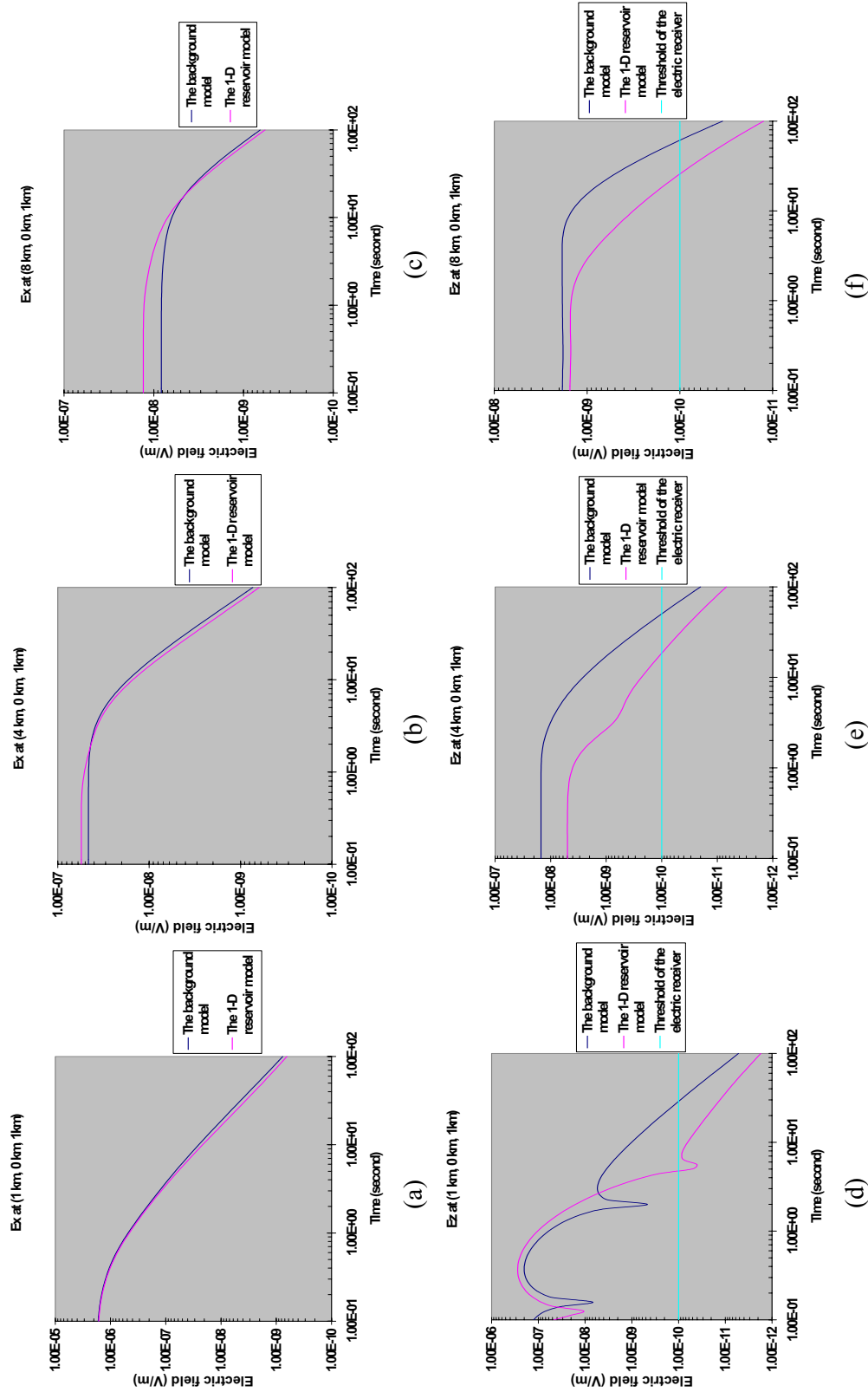


Figure 5.27. The in-line E_x and E_z responses at different receiver locations using the marine TDCSEM method.

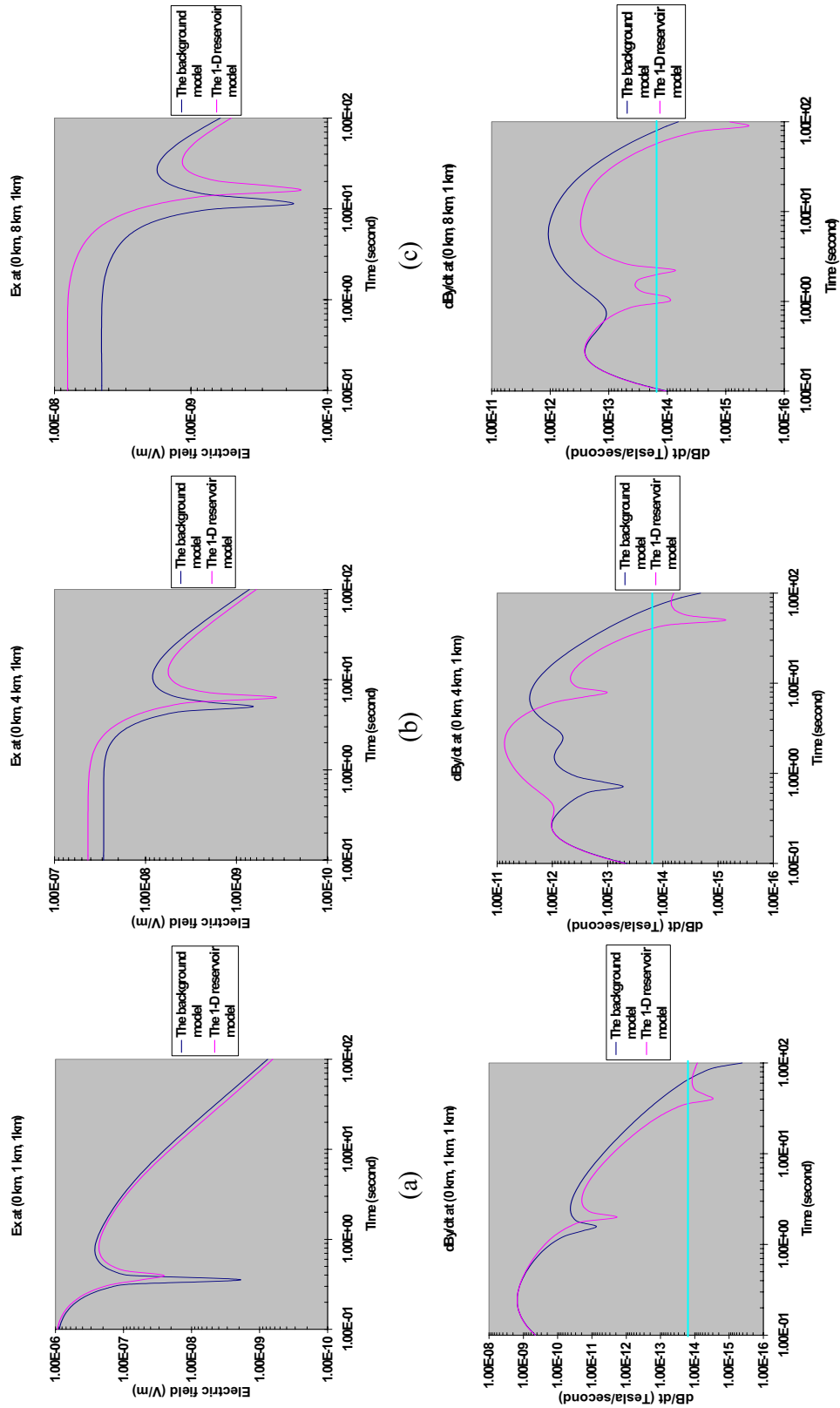


Figure 5.28. The broadside E_x and $dB_{Y/dt}$ responses at different receiver locations using the marine TDCSEM method. The aqua lines represent the receiver noise level.

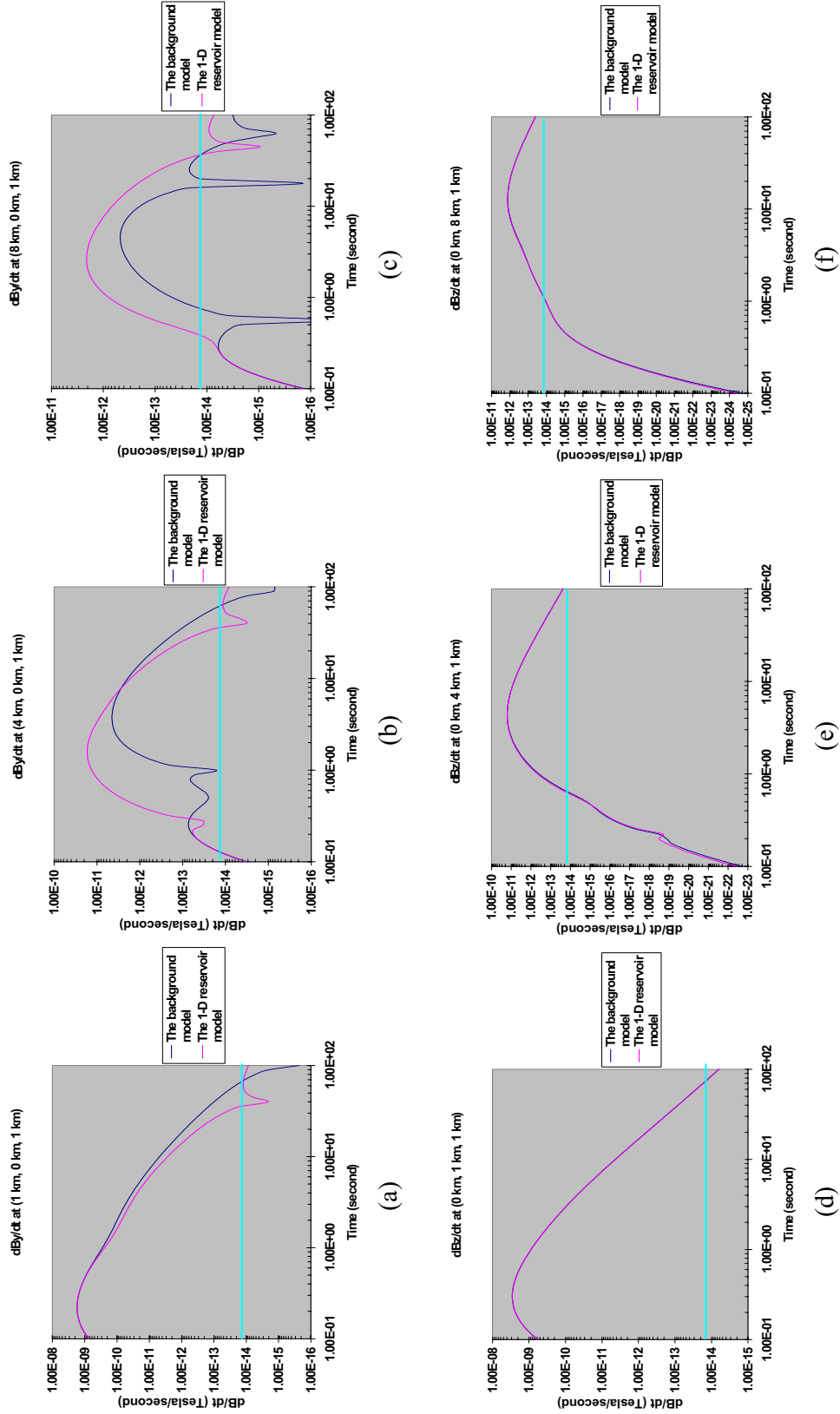


Figure 5.29. The in-line dB_Y/dt and broadside dB_Z/dt responses at different receiver locations using the marine TDCSEM method. The aqua lines represent the receiver noise level.

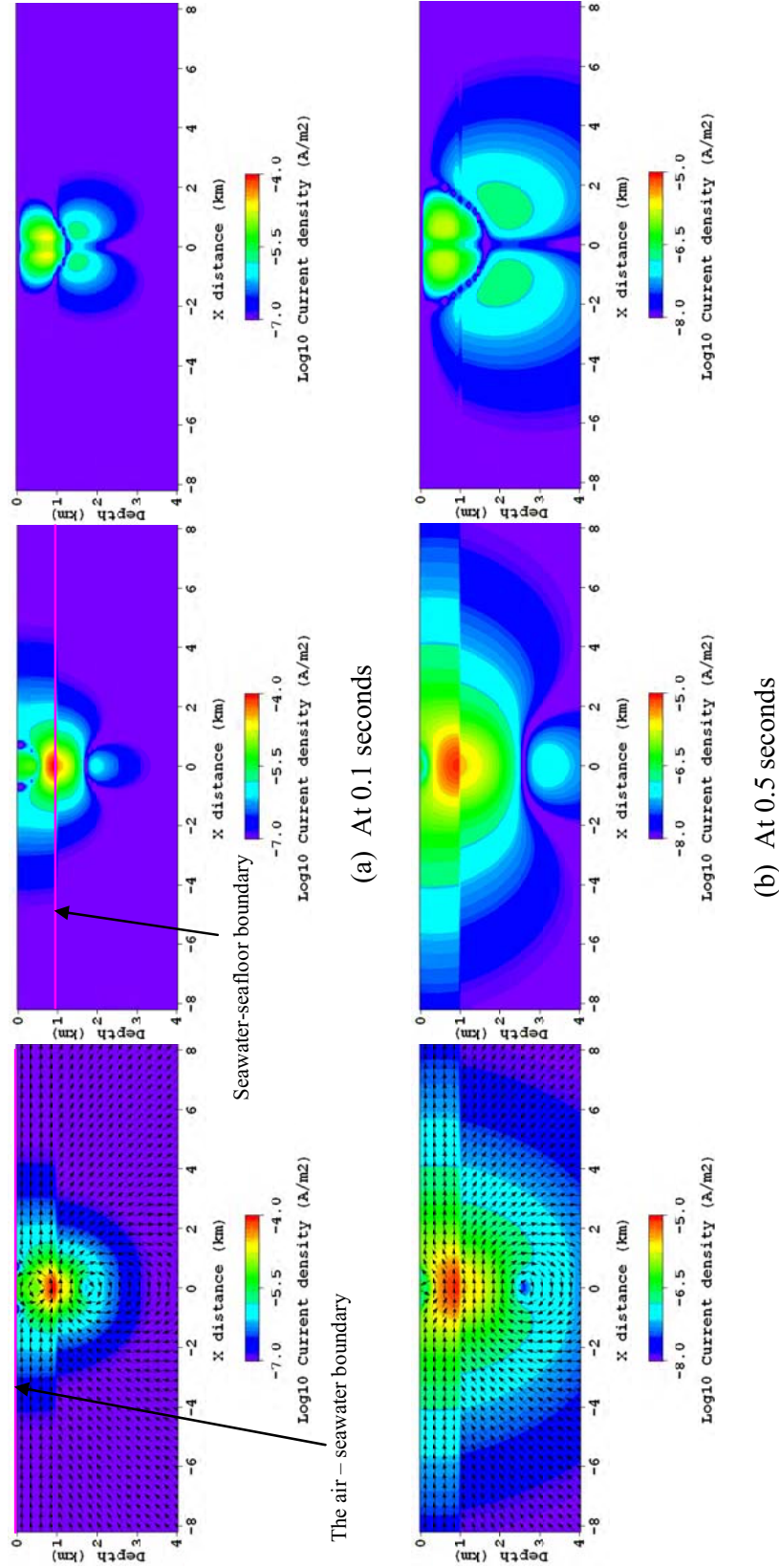
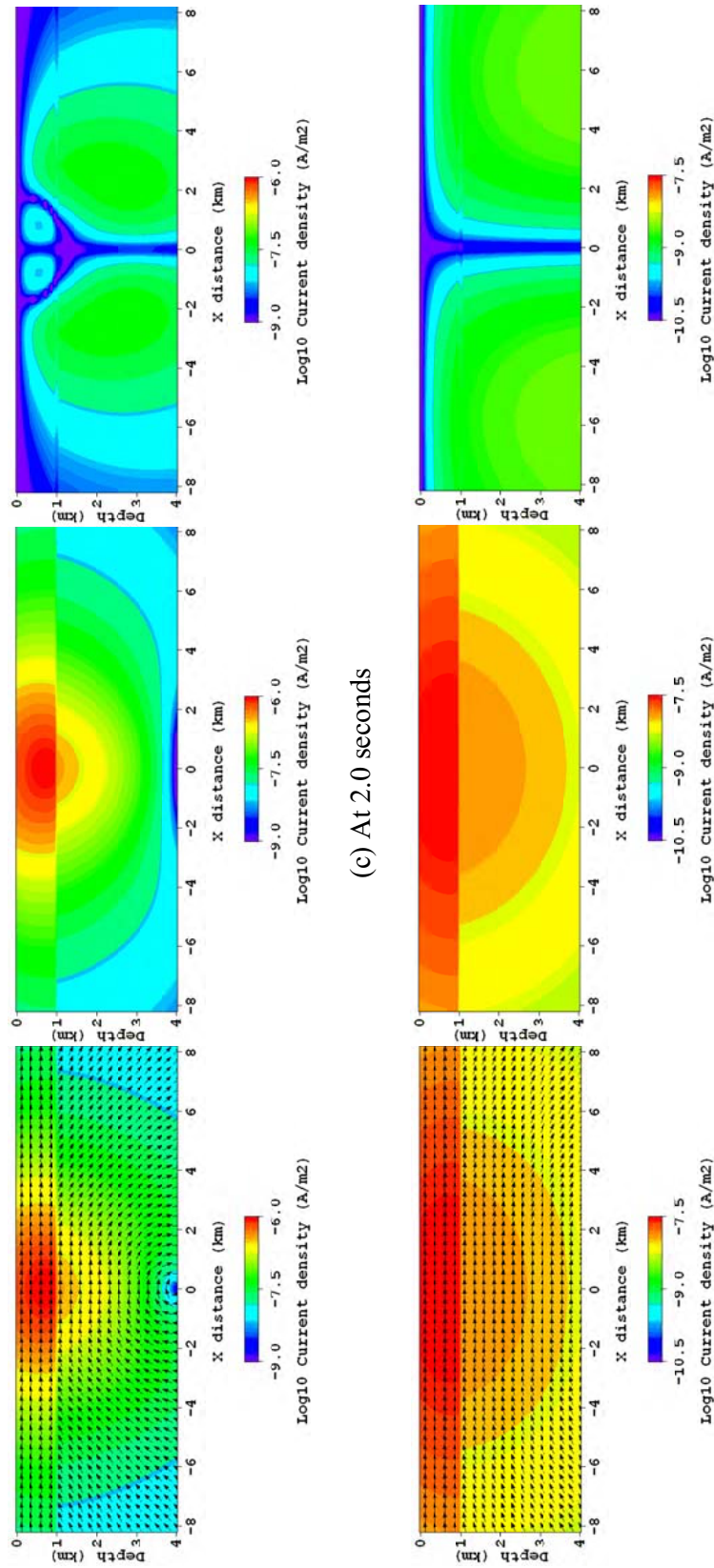


Figure 5.30. Current distribution snapshots at four different measurement times on the xz cross-section for the background model with a 250m long x-oriented time-domain HED source at (0 m, 0 m, 950 m). Total current density (left), horizontal current density (middle) and vertical current density (right).



(c) At 2.0 seconds

(d) At 20 seconds

Figure 5.30 Continued.

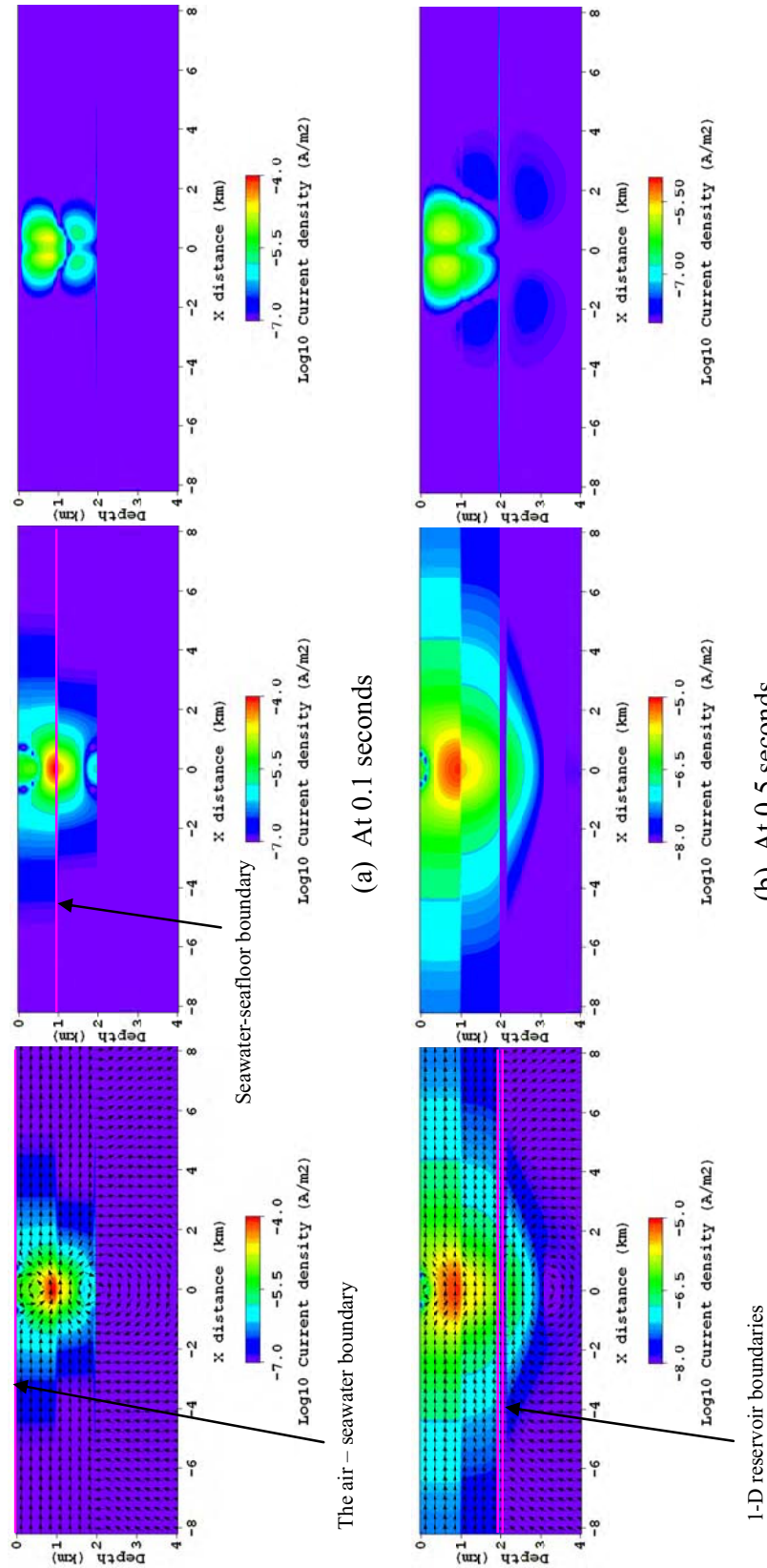


Figure 5.31. Current distribution snapshots at four different measurement times on the xz cross-section for the 1-D reservoir model with a 250m long x-oriented time-domain HED source at (0 m, 0 m, 950 m). Total current density (left), horizontal current density (middle) and vertical current density (right).